Title
Functionalized benzylamines from commercial kraft lignin

Journal
Chemical Engineering Journal, 532

ISSN
1385-8947

Authors
Dou, Chang
Yang, Minliang
Kumar, Nikhil
et al.

Publication Date
2026-03-01

DOI
10.1016/j.cej.2026.174287

Chemical Engineering Journal 532 (2026) 174287

Contents lists available at ScienceDirect

Chemical Engineering Journal

journal homepage: www.elsevier.com/locate/cej

Functionalized benzylamines from commercial kraft lignin

Chang Dou [a,b], Minliang Yang [b,c,d,e], Nikhil Kumar [c,f], Rolin A. Aguilar [a,b,g,1], Addison J. Hitt [a,b,h], Griffen Gonzalez [h], Corinne D. Scown [b,c,j,k], Kenneth L. Sale [c,f], Hemant Choudhary [c,i], Aaron M. Socha [b,h,*,2], Ning Sun [a,b,*]

[a] Advanced Biofuels and Bioproducts Process Development Unit, Lawrence Berkeley National Laboratory, Emeryville, CA, 94608, USA
[b] Biological Systems and Engineering Division, Lawrence Berkeley National Laboratory, Berkeley, CA, 94720, USA
[c] Joint BioEnergy Institute, Emeryville, CA, 94608, USA
[d] Department of Food, Bioprocessing and Nutrition Sciences, North Carolina State University, Raleigh, NC, 27606, USA
[e] Department of Biological and Agricultural Engineering, North Carolina State University, Raleigh, NC, 27606, USA
[f] Department of Biosecurity and Bioassurance, Sandia National Laboratories, Livermore, CA, 94551, USA
[g] Department of Chemistry, University of California, Berkeley, CA, 94720, USA
[h] Department of Biology and Chemistry, Queens University of Charlotte, 1900 Selwyn Avenue, Charlotte, NC, 28274, USA
[i] Department of Bioresource and Environmental Security, Sandia National Laboratories, Livermore, CA, 94550, USA
[j] Energy Analysis & Environmental Impacts Division, Lawrence Berkeley National Laboratory, Berkeley, CA, 94720, USA
[k] Energy & Biosciences Institute, Berkeley, CA, 94720, USA

ARTICLE INFO

Keywords:
Kraft lignin
Catalytic reduction
Mannich reaction
Phenolic benzylamines
Quantum chemistry simulations
Process analyses

ABSTRACT

Benzylamines are key intermediates in pharmaceuticals, agrochemicals, and polymers, but their conventional production relies on benzyl chloride - a petroleum-derived compound with high toxicity and energy demands. Lignin, accounting for up to 30% of plant biomass, is the largest renewable source of aromatic carbon on Earth. However, its highly complex and recalcitrant structure poses a major barrier to efficient conversion into high-value chemicals. Here, we developed a catalytic approach to convert commercial kraft lignin into phenolic benzylamines through selective depolymerization and subsequent functionalization. We systematically evaluated the effects of three alcohol solvents, formic acid (FA), and a ruthenium-on-carbon (Ru/C) catalyst on monophenol yield and selectivity. Up to 6.5 wt% monophenol yield was achieved using methanol (MeOH), FA, and Ru/C at 300 °C for 2 h. Quantum thermodynamic simulations based on the COSMO-RS model confirmed the superior solvation and reactivity of the MeOH + FA system, rationalizing observed product yield. The purified monophenolic products, primarily guaiacol and alkyl guaiacols, were then converted into functionalized benzylamines with >90% yield via a multicomponent Mannich reaction under mild conditions. Techno economic analysis (TEA) and life cycle assessment (LCA) underscore the importance of improving lignin depolymerization yields and expanding biorefinery scale. Solvent-only configurations outperform other options in both cost and emissions, with the methanol-only case performing the best ($105 /kg and 26 kg CO_{2e}/kg) at a large-scale facility. This study establishes a scalable, bio-based pathway for producing benzylamines from commercial kraft lignin, advancing lignin valorization and offering a sustainable alternative to produce petrochemical-based benzylamines.

1. Introduction

Benzylamines, important chemical intermediates for active pharmaceutical agents, also serve as versatile building blocks in the production of polymers, dyes, pigments, fertilizers, and pesticides [1–4]. Currently, benzylamines are derived solely from benzyl chloride, a petrochemical associated with high toxicity and air emissions [2,5,6]. Benzylamines derived from lignin offer a unique alternative to petroleum-based benzylamines. Phenolic, ether, and alkyl substituents can reduce the number of steps required for functionalization and

* Corresponding authors at: Biological Systems and Engineering Division, Lawrence Berkeley National Laboratory, Berkeley, CA, 94720, USA.
E-mail addresses: asocha@lbl.gov (A.M. Socha), nsun@lbl.gov (N. Sun).
[1] Present address: Stanford University, Department of Chemistry, 333 Campus Drive, Stanford, CA, 94305, USA.
[2] Present address: Institute for Chemical Technology of Materials, Technical University of Graz, Graz, 8010, Austria.

https://doi.org/10.1016/j.cej.2026.174287
Received 20 October 2025; Received in revised form 1 February 2026; Accepted 15 February 2026

facilitate downstream separation. This inherent structural diversity can enhance material performance and support cost-competitive, circular-bioeconomy pathways while reducing dependence on fossil-derived aromatic feedstocks. Specifically, lignin-derived benzylamines can act as antioxidants with alkyl substituents that impart hydrophobicity. Therefore, developing environmentally benign processes to produce phenolic benzylamines from renewable resources is highly desirable [1,7–9].

Lignin is a heterogeneous and polydisperse structural material comprising substituted phenylpropanoids that constitute 15–30% of plant biomass and is the largest known renewable source of aromatics [10,11]. Globally, pulp and paper mills produce approximately 100 million tons of lignin per year [12]; and the volume of lignin is expected to increase with the growth of the paper industry. Despite its substantial volume, less than 2% of industrial lignin is utilized for specific applications beyond low-value heating fuel [12,13]. Kraft lignin is a byproduct of kraft pulping, the dominant technology responsible for 90% of global pulp production [14]. In the kraft process, plant biomass (e.g., wood) is treated with sodium sulfide and hot sodium hydroxide to produce cellulose pulp, while the lignin-rich black liquor is burned to recover chemicals and generate energy [15]. The generation of kraft lignin often surpasses the design capacity of the recovery boiler, causing a bottleneck in the pulp production process [16]. Lignin extraction technologies (e.g., Lignoboost, LignoForce, and WestVaco) alleviate this issue by removing excess lignin before combustion, reducing the recovery boiler load and increasing pulp production capacity [14]. Recent advances in lignin extraction technologies have driven a 150% increase in global kraft lignin production from 2014 to 2018 [13,17,18]. All factors considered, the pulping industry now generates an excessive volume of kraft lignin.

To transform lignin into benzylamine feedstocks, an efficient, scalable lignin depolymerization method is required. Various lignin depolymerization techniques have been thoroughly reviewed, with the catalytic reduction processes being particularly effective for technical lignins (e.g., kraft lignin, lignosulfonate), biofuel-process derived lignins, and natural lignins [11,17–19]. Catalytic reduction of lignin occurs through benzylic alkoxylation, which breaks the polymer into smaller, soluble fragments (1.1–1.6 kDa) [20–22]. These fragments are then stabilized via reduction, typically facilitated by late transition metal catalysts (e.g., Ni, Ru, Rh, Pd, Cu, Fe, or Mo) in combination with either H_2 gas or hydrogen-donating solvents [23–25]. During the process, aryl or alkyl ether bonds, including β-O-4, 4-O-5 and α-O-4, are selectively cleaved while preserving aromaticity and suppressing repolymerization [23,24]. While H_2 gas is a common hydrogen source, approaches using in situ hydrogen generation from alcohols have shown great promise. The latter methods reduce reactor pressures, enhance monomer yields, and improve overall process economics [19,26,27]. Additionally, formic acid can serve as a hydrogen source, as it decomposes to H_2 and CO_2 at temperatures above 250 °C in the absence of a catalyst, or at lower temperatures with metal catalysis [28].

Various chemistries have been employed to introduce nitrogen groups into lignin-derived phenolic compounds [1,3,29]. Blondiaux et al. [2] recently showed the effectiveness of a Beckmann rearrangement in converting lignin-derived propyl guaiacol and propyl catechol into 3,4-dialkoxyanilines. As compared to a 7-step petrochemical synthesis from benzene, their 4-step bio-based method obviated the need for nitric acid. Another emerging method for production of amines from alcohols involves a hydrogen borrowing strategy [30] which has been applied to monolignols [8], β-O-4 dimers [9], and acidolysis lignin [31]. Benzylamines have also been made from benzyl alcohols using iron catalysts [32]. The Mannich reaction is a simple, effective, and widely accepted approach for preparing benzylamines from lignin monomers [33,34]. The Mannich reaction occurs when an aldehyde and a primary or secondary amine form a Schiff base that is attacked by an appropriate nucleophile to form a substituted amine product [35]. When phenolates are used as nucleophiles, the products are phenolic benzylamines. Previous work has shown the successful application of the Mannich reaction to produce lignin-based nitrogen containing compounds [2,36–38]. While several studies have focused on polymeric or oligomeric lignin amination [33,36,38–40], very few have explored the direct conversion of real lignin-derived monomers into benzylamines. This practical gap in applied lignin chemistry warranted further investigation.

The goal of this study was to produce phenolic benzylamines from lignin-derived aromatics using a Mannich multicomponent reaction strategy. Our previous works demonstrated the optimal production of phenolic benzylamines from oxidatively depolymerized kraft lignin [37,41,42]. However, low product yields resulting from complex lignin mixtures are still considered major obstacles for a lignin-to-amine process. To optimize the reaction parameters and improve monophenol yields, we compared three alcohol solvents - methanol (MeOH), ethanol (EtOH), and isopropanol (iPrOH) in combination with formic acid (FA) and ruthenium on carbon (Ru/C) to produce alkyl guaiacols. Monophenol yield and product distribution were analyzed to gain insight towards reductive depolymerization of lignin. Reactions using MeOH + FA and Ru/C synergistically achieved the highest yields, likely due to the higher solvation of lignin relative to the other alcohols. The COnductor like Screening MOdel for Real Solvents (COSMO-RS) predicted that the MeOH + FA mixture had the strongest interactions with lignin, confirming it as the superior reaction system for lignin. The purified lignin-derived monomers, such as guaiacol and alkyl guaiacols, were then subjected to Mannich reaction conditions that were first optimized using guaiacol model compounds. This process efficiently produced their corresponding phenolic benzylamines, demonstrating the successful functionalization of lignin-derived aromatic compounds. Techno-economic analysis (TEA) and life cycle assessment (LCA) were conducted to evaluate the overall process economics and commercial feasibility of a new bio-based benzylamine production process. This study presents a promising catalytic route for converting lignin into phenolic benzylamines, offering a sustainable and renewable alternative to petrochemical-based benzylamine production.

2. Experimental

2.1. Materials

The kraft lignin used in this study is BioChoice® lignin obtained from Domtar, Inc. (Fort Mill, SC, USA). BioChoice® lignin is extracted by acidification of filtered black liquor during the kraft pulping of southern pine using the LignoBoost® process [43]. Kraft lignin, as compared to natural lignin, is higher in C—C linkages but lower in β-O-4 ether bonds [14,44,45]. This highly condensed structure makes depolymerization more challenging, resulting in a relatively lower monomer yield compared to other lignin sources [19,46]. Regardless, a catalytic reduction process for kraft lignin could provide valuable insights into the reaction mechanism and be potentially applied to other lignins.

Ultimate (CHNS/O) analysis and chemical composition analysis were conducted following standardized protocols [47] (Table S1), and the results agreed with the previous study [48]. Methanol (MeOH), ethanol (EtOH), isopropanol (iPrOH), formic acid (FA), and ruthenium on carbon (Ru/C, 5% mass of Ru on activated carbon support) were used as received. Formaldehyde was used as a 37 wt% aqueous solution. Dimethylamine was used as a 2 M THF solution. Details of the chemicals are listed in Table S2.

2.2. Catalytic reductive depolymerization

Reductive depolymerization experiments were performed in a Parr Series 5000 Multiple Reactor System (Parr Instrument Co. Moline, IL, USA) that houses six 75 mL stainless-steel reactors. Each reactor is equipped with a magnetic stirrer and external heating unit. In a typical reaction, 200 ± 2 mg kraft lignin was loaded to 20 mL of alcohol solvent

(e.g., MeOH, EtOH, or iPrOH) in the reactor. 40 mg of Ru/C (5 wt% Ru loading on carbon) and/or 2 mL of FA were added under different scenarios [49]. Each reactor was purged with N_2 gas three times and then pressurized to 20 bar with N_2 gas [50]. The reaction temperature was increased to 300 °C and maintained for 2 h while stirring at 700 rpm. After the reaction, the reactor was quenched in an ice bath until it cooled to room temperature [27]. The reactor pressure was monitored and recorded throughout the process, including upon reaching the designated reaction temperature, at the conclusion of the reaction, and after cooling to ambient temperature (Fig. S1). Upon depressurization, decane was added into the reaction mixture as an analytical internal standard. The reaction contents were then vacuum filtered through a filter paper (Whatman Grade 5, 90 mm, Cytiv, Marlborough, MA) before analysis.

2.3. Mannich reactions with guaiacol model compounds and lignin-derived guaiacols

A series of Mannich reactions with guaiacol and alkyl guaiacol model compounds were performed to optimize conditions for the synthesis of lignin-derived benzylamines. Generally, 2 mmol of the guaiacol or alkyl guaiacol (1 eq) was solubilized in 1.0 mL EtOH, while dimethylamine (4 mmol, 2 eq) is condensed with formaldehyde (4 mmol, 2 eq) to form the iminium species. The solutions were combined into a 5 mL dram vial (15 × 45 mm) with a PTFE septa cap (Chemglass Life Sciences, Vineland, NJ) and heated in a laboratory oven at 80 °C for 22 h. The reaction contents were then dried in a vacuum centrifuge at 50 °C and subsequently analyzed by NMR. Mannich reactions on the depolymerized lignin products were carried out as follows: Approximately 320 mg of reductive depolymerized lignin sample was suspended in 20 mL of 0.1 M HCl and extracted with 2 × 10 mL ethyl acetate. The extract was concentrated in vacuo and chromatographed over 40–63 μm silica gel (Aldrich) using a 1 × 6 cm glass column, where 20 × 10 mL fractions were collected with 10:1 hexane:ethyl acetate as the mobile phase. Fractions #3–6 (~10 mg each) were combined based on GC–MS similarity, and contained methyl guaiacol, ethyl guaiacol, and propyl guaiacol in approximately 1:4:10 ratio. No appreciable amount of guaiacol was obtained in the purification, but traces of guaiacol were observed in latter fractions using GC–MS. Approximately 1.0 mg (~7 μmol) aliquots of the combined fractions were reacted using the reaction conditions described for the model compounds. As a control, a mixture of model compounds (1:4:10 of methyl guaiacol, ethyl guaiacol, and propyl guaiacol) was subjected to the same reaction conditions.

2.4. Product analysis and characterization

2.4.1. Depolymerized lignin product analysis

Product analysis of reductive depolymerized lignin was performed using an Agilent 6890 N gas chromatography (GC) system coupled with a 5973 N mass spectrometry (MS) detector, equipped with a DB-5MS column (30 m × 0.25 mm × 0.25 μm, Agilent Technologies, Santa Clara, CA). Helium was used as carrier gas with a constant flow rate of 1 mL/min. At an inlet temperature of 280 °C, 1 μL auto-injections were made with a split ratio of 20:1. The GC oven temperature was programmed to hold at 80 °C for 5 min, followed by a ramp of 5 °C/min to 200 °C. From 200 °C, the temperature was increased at a rate of 20 °C/min to 300 °C and held for 8 min. The ion source was maintained at 280 °C with a solvent delay of 3.5 min. MS signal was recorded at a total rate of 20 Hz. Six monophenols: guaiacol, methyl guaiacol, ethyl guaiacol, propyl guaiacol, eugenol, and isoeugenol, were quantified using response factors determined by respective analytical standards with decane as the internal standard.

2.4.2. Mannich reaction product characterization

Samples from Mannich reactions were analyzed in a Thermo Trace 1300 GC–MS (Waltham, MA) equipped with a Thermo TG-SQC column (30 m × 0.25 mm × 0.25 μm) using helium as carrier gas at 1 mL/min. The column temperature was held at 100 °C for 1 min, then ramped to 325 °C at a rate of 10 °C/min, and finally maintained at 325 °C for 3 min. The MS was set at positive ion electron impact mode from *m/z* 50–650. Retention times and *m/z* ratios of lignin-derived benzylamine products matched those obtained from reactions using authentic standards (see SI for GC–MS spectra). The reaction mixtures were dried in a vacuum centrifuge at 50 °C and analyzed directly by a 60 MHz NMR (Anasazi Instruments, Inc., New Palestine, IN) using $CDCl_3$ (Cambridge Isotopes). Tetramethylsilane (TMS) was used as an internal standard for chemical shift referencing. All reactions with alkyl guaiacols gave quantitative yields of pale-yellow oils (see SI for ^1H and ^{13}C NMR spectra).

2.5. Quantum chemistry modeling

Turbomole (TmoleX) was used to optimize the molecular structures of lignin, MeOH, EtOH, iPrOH, and FA. The COntinuum Solvation MOdel for Real Solvents (COSMO-RS) was used to calculate the chemical potential of solute-solvent systems. COSMO-RS is a hybrid solvation model that uses quantum chemistry and statistical thermodynamics to compute the chemical potentials that were used to predict the different thermodynamic properties [51]. The calculations were carried out using the def-TZVP "triple-zeta valence polarized" basis set and the Becke-Perdew (BP86) exchange-correlation functional (SCF convergence of 1×10^{-6} Hartree with 500 cycles) [52,53]. The output from COSMO-RS was then imported into BIOVIA COSMOtherm (COSMOtherm 2023 version 23.0.0) for calculating the thermophysical properties of the lignin and solvent mixtures (83 [54]. Fig. 1 shows the lignin polymer structure used in the calculation of thermophysical properties for alcohols and their respective mixtures with formic acid. The detailed discussion for calculating the activity coefficient ln(γ) was described previously [55,56] and relates to the chemical potential (μ_{lignin}) of the lignin as expressed in Eq. (1):

$$In(y) = \frac{\mu_{solvent} - \mu_{lignin}}{RT} \quad (1)$$

where:

- $\mu_{solvent}$ is the chemical potential of the solvent.
- μ_{lignin} is the standard chemical potential of the lignin.
- R is the ideal gas constant.
- T is the absolute temperature (K).

The transfer energy from the gas phase to the liquid phase (i.e., the Gibbs free energy of solvation) was defined in Eq. (2) [57]:

$$\Delta G_i^{solv} = G_i^S - G_I^{Gas} = E_i^{COSMO} + \mu_i^S - E_i^{Gas} \quad (2)$$

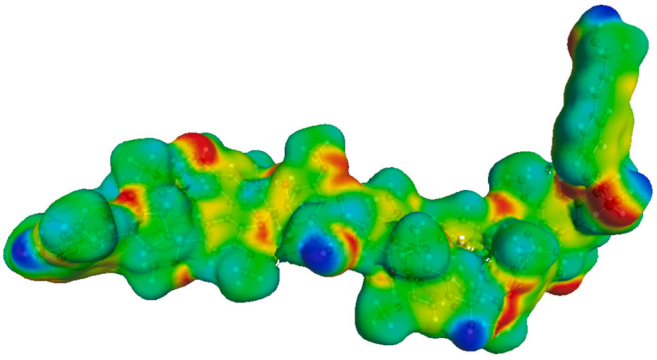

Fig. 1. The COSMO-RS generated lignin polymer model structure (DP = 26) with different monomeric units and linkages was used in the present study (detailed structure refer to Fig. S2).

where E_i^{Gas} and E_i^{COSMO} are the quantum chemical total energies of the molecule in the gas phase and in the COSMO conductor, respectively. The COSMO-RS method was used to predict the thermodynamic properties of lignin solvation and validate it using the experimental results in multiple previously published studies [54–57]. According to the solid-liquid equilibria assumptions [58], the activity coefficient characterizes lignin solvation in the respective alcohols by measuring the lignin-solvent interaction. The solvents were sorted according to their dissolving capacity and arranged with a high dissolving power of lignin (i.e., $\ln(\gamma) \ll 0$). In the present study, COSMO-RS model-based calculations for solvation were performed to understand the effects of different alcohol protic solvents such as MeOH, EtOH, iPrOH, FA, and their solvent mixtures that help catalysts to give a higher yield of monophenols from reductive catalytic fractionation of lignin.

2.6. Techno-economic analysis and life-cycle assessment

The process model of the lignin-based benzylamine production was developed in *SuperPro Designer v12* (Figs. 2 and S3). Key assumptions are listed in Table S3. The benzylamine facility starts from kraft lignin receiving and short-time onsite storage, lignin depolymerization and separation, to benzylamine production via Mannich reaction. Consistent with our experiment, BioChoice® lignin (typically contains 65% solids) from Domtar is used as the feedstock with the assumed selling price of $1/kg. After kraft lignin is transported to the facility, it goes through the drying process to remove excess water and is stored for a short period of time onsite. Afterwards, the dried lignin is sent to the depolymerization process under different experimental scenarios tested in this study: three alcohol solvents, with and without Ru/C, with and without FA. The loading rates of lignin, Ru/C, and FA are 1%, 0.2%, and 10% *w/v*, respectively. Regardless of the solvent scenarios, the reaction conditions are applied at 300 °C for 2 h under initial 20 bar N_2. Solvents used in lignin depolymerization are recycled at a rate of 99%. Afterwards, the slurry from the reactor goes through the separation process to separate depolymerized lignin residue from the stream. Given large amounts of depolymerized lignin residue from this process and their potential future applications in markets, we consider it as a by-product from the benzylamine facility with the same selling price ($1/kg) as kraft lignin. Guaiacols are then processed to benzylamines via a Mannich reaction using dimethylamine and formaldehyde. At 70 °C for 20 h, and Mannich reaction the final yield is set to be 95%. We assume formaldehyde will be recycled at 90%. The final products are sent to the downstream separation stage and stored on-site before selling to the market.

We developed process models on two scales: 1) state-of-art scale of 75 t of kraft lignin per day, and 2) large scale of 750 t of kraft lignin per day. State-of-art scale is chosen based on Domtar's previous LignoBoost plant size, and large scale is added to explore potential future scenarios in costs and carbon footprint reduction. We assume the benzylamine facility will operate 7920 h per year with a plant life of 30 years. After performing mass and energy balance, we calculated minimum benzylamine selling price (MSP in $/kg) via discounted cash flow analysis using a 10% discount rate. Additional assumptions were aligned with the National Renewable Energy Laboratory (NREL) report [59]. Sensitivity analysis was performed on key input parameters to explore their potential impacts on final costs. We further quantified the carbon footprint per kg of benzylamine on a large-scale facility through life-cycle assessment. Mass and energy data were obtained directly from the techno-economic models developed in *SuperPro Designer*. Background data were collected from various sources such as the Greenhouse Gases, Regulated Emissions, and Energy use in Technologies (GREET), EcoInvent, and peer-reviewed articles. The system boundary starts from kraft lignin production, lignin depolymerization to lignin-based benzylamine production. Similar to TEA, uncertainty analysis of LCA was performed to capture the variations in each input parameter.

3. Results and discussions

3.1. Reductive depolymerization of kraft lignin

3.1.1. Monophenol product yield

To evaluate the effect of Ru/C and FA in three alcohol solvents (i.e., MeOH, EtOH and iPrOH) on lignin depolymerization, a total of six lignin derived monophenols were quantified. Across all experiments, four major guaiacol products were observed (guaiacol, methyl guaiacol, ethyl guaiacol, propyl guaiacol) along with two minor products (eugenol and isoeugenol) (Fig. S4). This differs from other catalytic alcoholysis research, which report more complex product distributions [60]. This is likely due to the following three factors. First, the lignin source plays a significant role in determining product distribution [19,61,62]. The kraft lignin used in this study, BioChoice® Lignin, is extracted from southern pine through the kraft pulping process. Softwood lignin primarily contains guaiacyl units, which generally yield fewer monophenolic analogues compared to lignin from hardwoods or herbaceous sources. Additionally, kraft lignin is known to be more condensed and less reactive than lignins extracted via other processes, resulting in fractionation to a less diverse range of products [63]. Second, the workup procedure also influences the product profile [64,65]. Unlike many previous studies, the lignin products in this work were analyzed directly after the reaction, without concentrating the oil for mass determination. This approach minimizes post-reaction transformations, such as condensation or oxidation. Third, the choice of catalyst plays a role in shaping the product composition. Ru/C, known as an effective heterogeneous catalyst for reductive lignin depolymerization, has been applied in many studies, yet the product profile resulting from Ru/C differs from other catalysts [19,66]. Notably, the relatively simpler products observed in this study could benefit product separation - a

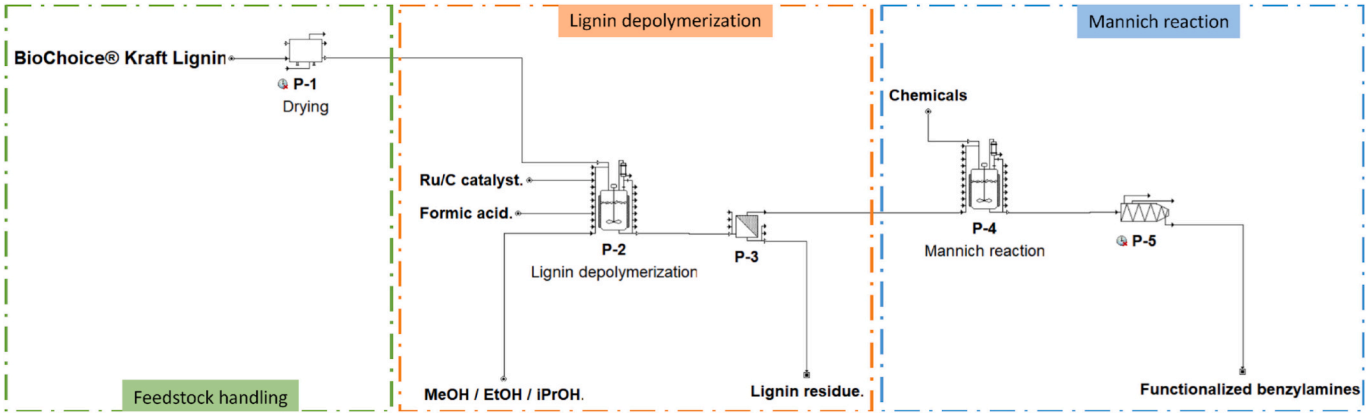

Fig. 2. Simplified process diagram of the lignin based benzylamine facility (refer Fig. S3 for complete process).

major challenge in lignin valorization [67].

Fig. 3 compares total monophenol yield across three alcohol solvents under four scenarios, i.e., alcohol solvent only, alcohol solvent with FA, alcohol solvent with Ru/C, and alcohol solvent with both FA and Ru/C. In the solvent-only scenarios, MeOH gave higher monophenol yields (4.9 ± 0.1%) as compared to EtOH (3.8 ± 0.2%) and iPrOH (3.9 ± 0.2%). Similar trends were observed for the other three conditions, where the highest monophenol yields were achieved in MeOH followed by EtOH and iPrOH. These findings align with previous studies that report higher delignification and lignin oil yield when using MeOH as a solvent compared to EtOH and iPrOH [20,68,69]. This difference is at least partially attributed to the greater polarity and higher lignin solubility of MeOH, compared to EtOH and iPrOH. Higher solvent compatibility allows MeOH to penetrate the matrix of lignin and fragment the lignin [68,69]. A similar trend, relating alcohol type to lignin depolymerization, was reported with other transition metal catalyst systems [19,49,70].

MeOH is also the most acidic alcohol tested (MeOH pKa = 15.5, EtOH pKa = 16.0, iPrOH pKa = 16.5) [71] and the equilibrium of proton dissociation favors formation of the alkoxide, which has two roles in the proposed mechanism (Scheme 1). In step *i*, upon water loss under acidic conditions, a stable benzylic carbocation forms at the α-position. The alkoxide nucleophile attacks the α-position (step *ii*), effectively protecting the lignin from recondensation reactions. In step *iii*, the alkoxide ion serves as a base to remove the β proton, forcing the elimination of formate. The result is a higher concentration of the unsaturated ether that is reductively cleaved to form monophenolic products. Additionally, alcohol solvents with more hydroxyl groups are associated with better lignin dissolution [20] and MeOH contains the greatest "hydroxyl density" compared to the other alcohols tested. In addition to MeOH being the best lignin solvent and strongest acid among the alcohols tested, its size allows for the least hindered nucleophilicity. FA, serving as an in-situ hydrogen source during metal-catalyzed reductive lignin depolymerization, was applied to all three alcohol solvent systems. FA alone increased the monophenol yield by 14% when MeOH was used as the solvent (Fig. 3). This is consistent with what was observed in other studies and can be attributed to FA decomposition at elevated temperature [19]. Serving as a hydrogen donor, FA facilitates reductive lignin depolymerization by stabilizing the depolymerized products and suppressing re-polymerization reactions [72–74]. In addition to supplying a proton to a hydroxyl group, gas phase FA is also known to provide a hydrogen radical environment [75]. In the presence of alcohols, hydrogen radicals can produce hydrogen gas. Additionally, as a saturated carboxylic acid, FA can participate in a bimolecular tautomeric mechanism by coordinating its carbonyl and OH groups with the β proton and a hydroxyl groups, respectively [76]. While not shown in Scheme 1, this hydroxyl-assisted hydrogen transfer mechanism may be responsible for the formation of isoeugenol as a minor product. At elevated temperatures, alcohols also act as hydrogen donors via decomposition, contributing to lignin depolymerization [77].

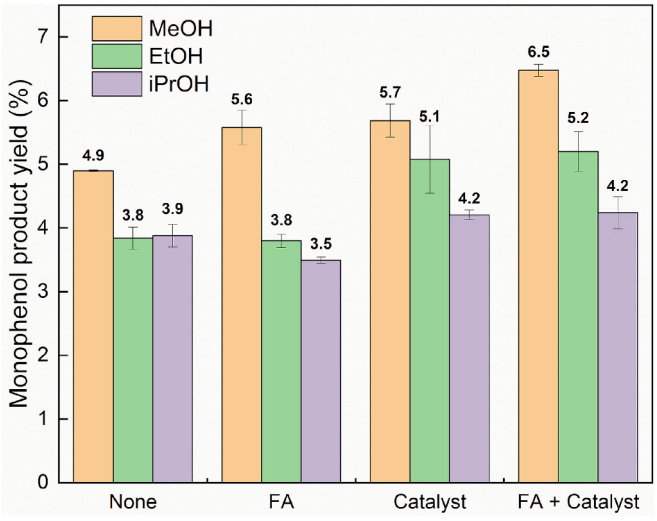

Fig. 3. Effect of different alcohol solvents on the product yields (wt%) of monophenols with and without the presence of FA and/or Ru/C. "None" indicates the use of the alcohol solvent alone; "FA" indicates formic acid in the solvent; "Catalyst" indicates the presence of Ru/C in the solvent; and "FA + Catalyst" indicates the combination of both formic acid and Ru/C in the solvent.

Researchers have found that reductive catalytic fractionation of lignin under acidic conditions leads to a resonance-stabilized benzylic carbocation that is alkoxylated by the solvent (Scheme 1 steps i-ii), preventing repolymerization at the alpha position [27,50,78,79]. Monophenol product yields increased in the order of MeOH > EtOH > iPrOH, likely due to respective nucleophilicities and steric effects of the alcohols. Stahl and coworkers [78] reported the FA induced depolymerization of lignin, and concluded that lignin is formylated at the γ aliphatic hydroxyl position (Scheme 1 step ii). Using Density Functional Theory (DFT) calculations, an elimination mechanism was proposed by Qu et al. [79] to support proton abstraction from the β position of the formylated lignin. Oregui-Bengoechea et al. [50] extended FA-induced catalytic reduction methods to enzymatically hydrolyzed eucalyptus lignin, and suggested the rate-limiting elimination step (Scheme 1, step *iii*) is facilitated by the conjugate base of the alcohol solvent. Our results support these mechanisms by demonstrating reductive ether cleavage to form propyl guaiacol at temperatures >250 °C [80]. In accord with equilibrium theory, subcritical reaction conditions allow acidic and basic properties of a protic solvent to be exploited [81]. Additionally, pKa values decrease with increasing temperature during endothermic reactions, such as those involved in lignin depolymerization [82].

When Ru/C was applied to all three solvent systems, it increased total monophenol yield by 16%, 30%, and 8% in MeOH, EtOH, and iPrOH, respectively, compared to solvent-only scenarios. Ru/C, characterized by highly dispersed active metal particles, is known to facilitate the decomposition of alcohols, generating more hydrogen for reduction of lignin linkages and side chains [74,83].

Greater monophenol yields were observed across all three alcohol solvents in the combined presence of Ru/C and FA (Fig. 3). In particular, the combination of FA and Ru/C in MeOH exhibited synergistic effects on lignin depolymerization, yielding more monophenol than when either RA or Ru/C was used alone. When both Ru/C and FA were added, 32% more monophenols were obtained, as compared to MeOH alone. Reactions with MeOH, FA, and Ru/C display the highest overall yields of phenolic monomers, reaching 6.5%, followed by EtOH (5.2%) and iPrOH (4.2%). The trend of monophenol yields observed across different alcohols was consistent with other studies using Ru/C and FA with hardwood organosolv lignin [60]. Ru/C promotes hydrogen evolution from FA; and is considered more effective for lignin reduction than using alcohols as the sole hydrogen source [83]. According to Huang [84], hydrogen radicals are generated in situ from FA, and absorbed onto the metal catalyst support surface where they contact and reduce lignin.

The addition of FA, regardless of the presence of Ru/C, did not change the total monophenol yields in EtOH or iPrOH. It is noteworthy that lignin depolymerization kinetics differs due to the interactions between FA and alcohols. The rate of FA decomposition in MeOH is higher than in EtOH or iPrOH, resulting in more hydrogen available for in-lignin depolymerization [50]. In another study, Riaz et al. 2018 [46] reported that the addition of FA suppresses the decomposition of EtOH by nearly 40%.

3.1.2. *Monophenol product selectivity*

In addition to the total monophenol yield, individual monophenols were quantified to study the influence of solvent, FA, and Ru/C on product selectivity. The absolute yield of individual monophenols is summarized in Table S4. Figs. 4 and S4 illustrate the distribution of

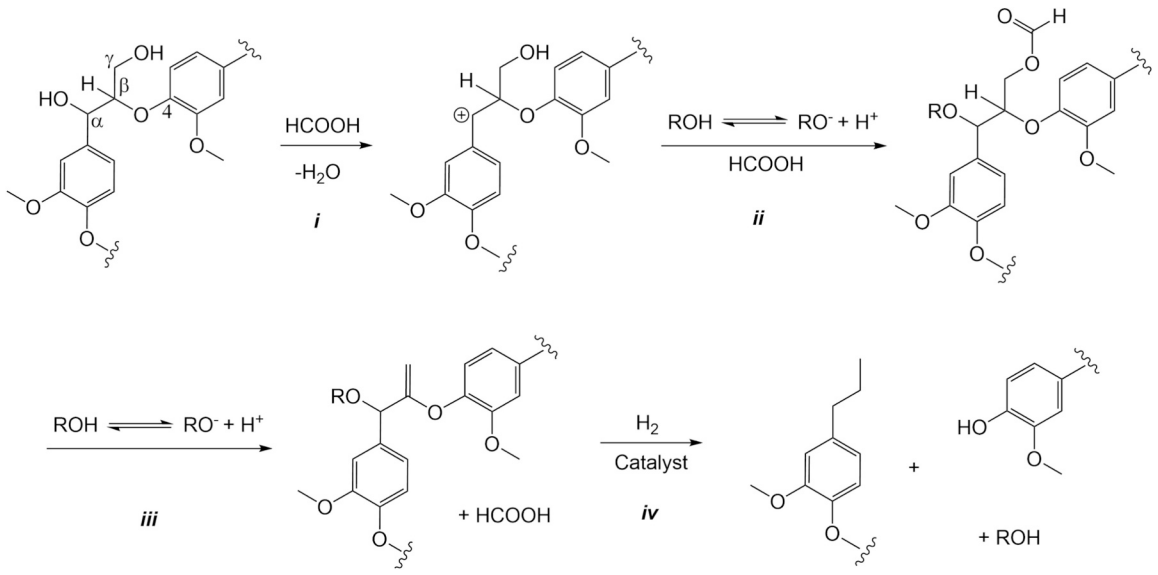

Scheme 1. Proposed mechanism of reductive catalytic lignin depolymerization in alcohol (adapted from Ref. [50]), showing *i*: formylation, water loss and formation of benzylic carbocation, followed by *ii*: alkoxylation, *iii*: β deprotonation and elimination, and *iv*: catalytic reduction of C—O and C═C.

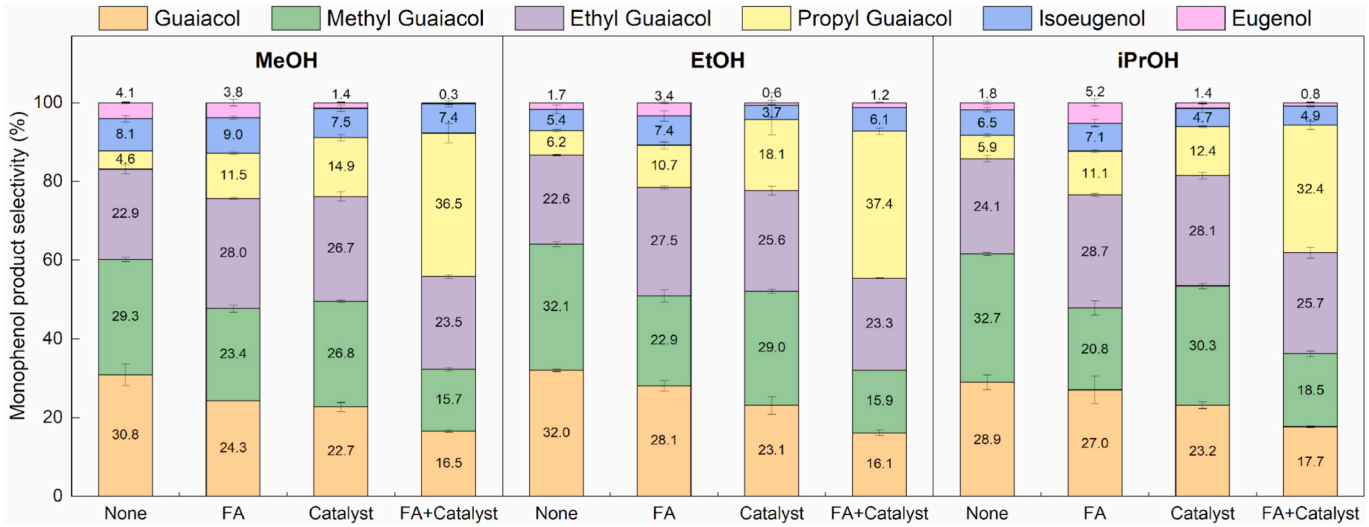

Fig. 4. Comparison of product distribution across different alcohol solvents with and without FA and/or Ru/C (labeled as Catalyst), refer Table S4 for the absolute individual monophenol yields.

monophenols, which shows a very little difference across the alcohol solvents. In solvent-only conditions, the reactions were the most selective towards guaiacol (28.9–32.0% of products) and methyl guaiacol (29.3–32.7% of products), followed by ethyl guaiacol (22.6–24.1%) and propyl guaiacol (5.4–8.1%). It is important to note the type of alcohol applied in the reaction does not correlate with the alkyl-group substitution on guaiacol; for example, iPrOH does not lead to higher yields of propyl guaiacol [85]. FA and Ru/C showed more significant impacts on the monophenol selectivity compared to the solvent [68]. Taking MeOH as an example, adding FA reduced the compositions of guaiacol (from 30.8% to 24.3%) and methyl guaiacol (from 29.3% to 23.4%), but increased the compositions of ethyl guaiacol (from 22.9% to 28.0%) and propyl guaiacol (from 4.6% to 11.5%). A similar effect was observed when Ru/C was applied in MeOH, where guaiacol and methyl guaiacol yields decreased to 22.7% and 26.8%, respectively, whereas yields of ethyl guaiacol and propyl guaiacol increased to 26.7% and 14.9%, respectively. The impacts were compounded when both FA and Ru/C were employed in MeOH, suppressing the compositions of both guaiacol and methyl guaiacol to 16.5% and 15.7%, respectively, and boosting the composition of propyl guaiacol to 36.5%. The same trends were observed for EtOH and iPrOH. For the first time, we report a correlation between product selectivity using FA and catalyst, demonstrating tunable monophenol product distribution aimed at longer alkyl chain guaiacols by adding FA and Ru/C.

Besides affecting alkyl chain length of the monophenols, the presence of FA and Ru/C are also found to influence the composition of eugenol. FA alone increased the eugenol composition in EtOH and iPrOH. In contrast, Ru/C decreased eugenol yields in reactions with and without FA across all solvent systems. Eugenol reduction to propyl guaiacol has been reported in hydrothermal ethanolic systems using Pt/C [86]. FA and Ru/C did not show much impact on the composition of isoeugenol as its double bond is stabilized through conjugation to the aromatic system.

Reductive depolymerization of kraft lignin has been investigated in many studies [17,19,87,88], with most reports emphasizing overall bio-oil yield, whereas precise quantitative data on monophenol product

yields are less frequently presented. Depending on the reaction conditions, selection of catalyst, solvent, and hydrogen source, the monophenol product (phenols, guaiacols, and catechols) yield varied from 2.9 to 28.5 wt% [19,87]. While our total monophenol yields are in the lower range compared to other kraft lignin reductive depolymerization studies, our guaiacol yields are among the highest literature values (1.75–7.8 wt%) [89,90].

3.2. Analysis of lignin interaction with solvent systems using the COSMO-RS model

The activity coefficient ln(γ) and Gibbs free energy of solvation (ΔG_{solv}) are critical thermodynamic parameters used to understand solvation of lignin and were calculated using the COSMO-RS model of the different alcohol solvents and their alcohol + FA solvent mixtures. Fig. 3A–B show the ln(γ) and ΔG_{solv} for lignin in the pure alcohols and in

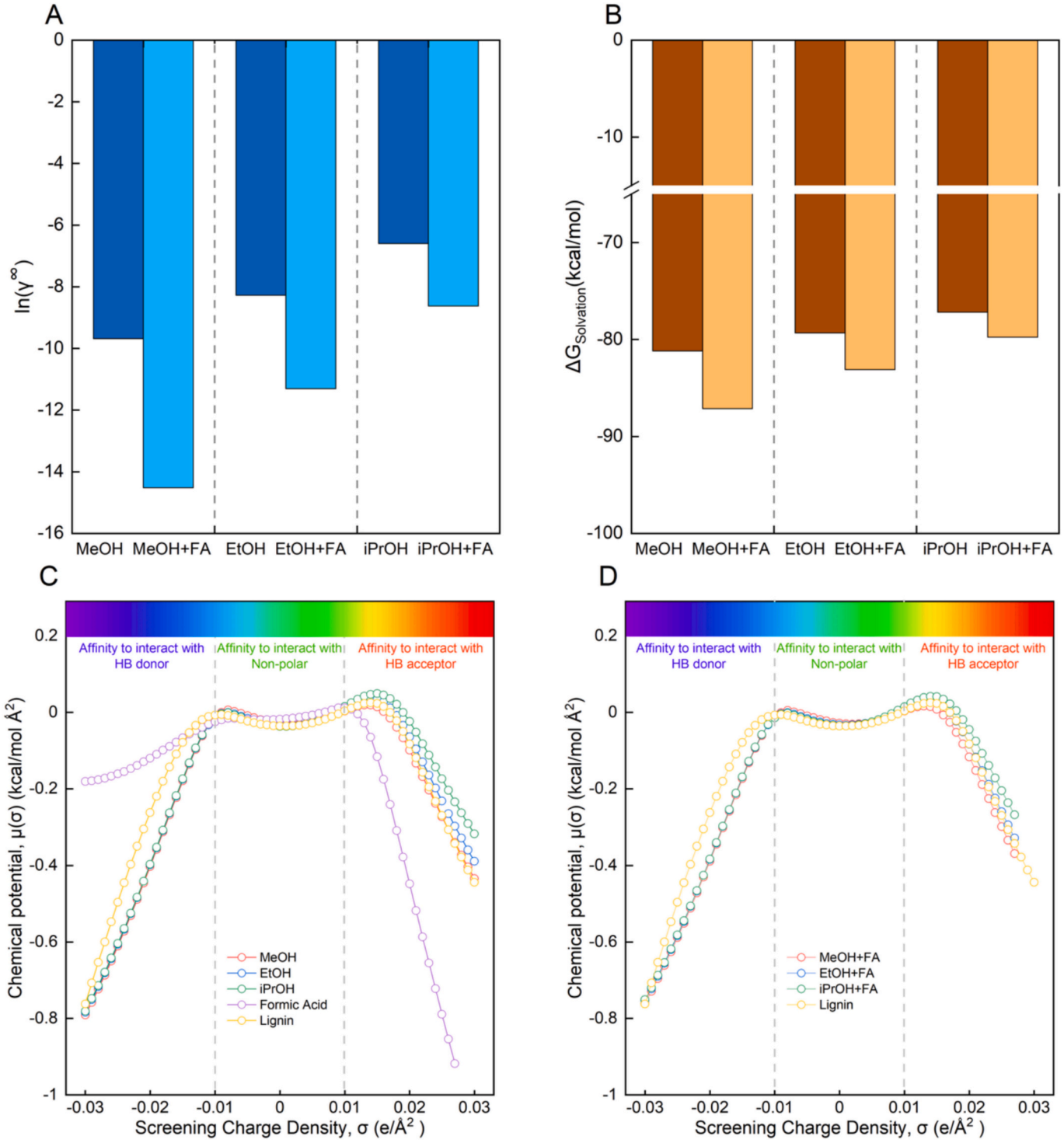

Fig. 5. A) Activity coefficients for lignin in individual alcohol solvents and their alcohol + FA mixtures at 300 °C, B) Gibbs free solvation energies for lignin dissolution in individual alcohols and formic acid and their mixtures, C) COSMO-RS model calculated sigma (σ)-potentials of lignin with individual alcohol solvents. D) COSMO-RS-calculated σ-potentials of lignin with alcohol + FA mixtures.

mixtures of 95% alcohol and 5% FA. The ln(γ) for protic alcohols and alcohol + FA mixtures were used to understand differences in lignin-solvent interactions. The MeOH + FA solvent system exhibited a more negative value of ln(γ), indicating stronger interactions with lignin, compared to EtOH + FA and iPrOH + FA systems (Fig. 5A). Alcohols act as protic solvents, and adding FA made them more likely to interact with lignin, as evidenced by increased activity coefficients (Fig. 5A). To understand the effect of temperature, activity coefficients were calculated from 25 to 300 °C and increased with temperature, as shown in Fig. S5. A similar trend of solvation was observed across different temperatures for ionic liquids in alcohols and ketones at elevated temperatures compared to ambient conditions, as published in earlier studies [91]. Fig. 5B shows the Gibbs free energy of solvation (ΔG_{solv}) for lignin in the individual alcohols and in the alcohol + FA solvent systems. The MeOH + FA solvent system exhibited the lowest ΔG_{solv} (−87.13 kcal/mol), indicating stronger lignin solvation compared to EtOH + FA and iPrOH + FA systems, which was consistent with predictions based on ln(γ) values (Fig. 5A).

To gain insights into the polarity and reactivity of lignin with different solvent systems, chemical potentials (σ) of lignin model compounds, alcohols, and alcohol + FA systems were calculated using the COSMO-RS method. The σ-potential quantifies the molecule's affinity for surfaces of varying polarity [92], providing valuable information about lignin interactions with itself and with different solvents. The σ-potential was divided into three regions based on the surface screening charge density (Fig. 3C–D): the negative charge density region where it prefers to interact with H-bond donors ($\sigma < -0.01$ eÅ^{-2}), the positive charge density region where it prefers to interact with H-bond acceptors ($\sigma > +0.01$ eÅ^{-2}), and a non-polar charge density region (-0.01 eÅ$^{-2} < \sigma < +0.01$ eÅ^{-2}). The σ-potential of lignin, $\mu(\sigma)$, was negative in both the negative and positive charge density regions (Fig. 5C–D), indicating that lignin interacts with both negative and positive polar surfaces (i.e., lignin interacts with both H-bond donors and acceptors in the solvent). Fig. 5C reveals that FA has a less negative μ(σ) compared to alcohols in the positive charge density region (SCD: $\sigma > +0.01$ Å^{-2}) and a more negative μ(σ) in the negative charge density (SCD: $\sigma < -0.01$ Å^{-2}), which indicates it more strongly interacts with H-bond acceptor sites of lignin (i.e., ether bonds, carbonyl groups, and hydroxyl groups). In individual solvents, MeOH had more negative chemical potential, and μ(σ) decreased with increased alkyl chain length. Similarly, in alcohol + FA systems, the chemical potential μ(σ) of the MeOH + FA system was the most negative and its affinity to interact with H-bond acceptor sites available in lignin increased with the addition of FA. The more negative chemical potential μ(σ) of the MeOH + FA in this region indicates it has a higher affinity for interacting with lignin through H-bonding interactions compared to EtOH + FA and iPrOH + FA (Fig. 5D). Thus, MeOH + FA, with its high H-bond donor strength and substantial H-bond acceptor complementarity, emerged as the most potent lignin solvent. In comparison, the iPrOH + FA mixture exhibited lower H-bond donor character and limited H-bond acceptor potential, suggesting a reduced efficiency in solubilizing lignin. However, this mixture may offer advantages in controlling the extent of undesired side reactions.

We also hypothesize that the highest monophenol yields are attributable to superior solvency, observed in MeOH (and MeOH + FA) systems. However, the quantum predictions did not fully explain the yield differences between EtOH and iPrOH in the absence of the catalyst. This result is likely due to greater ease of oxidation, and hence greater hydrogen production from the latter alcohol [93]. Hydrogen dissociation from the central carbon atom of iPrOH leaves a secondary alkyl radical which is more stable compared to the primary alkyl radical formed upon hydrogen loss from EtOH. By means of comparison, iPrOH is also known to produce more hydrogen than *n*-propanol [94].

3.3. Mannich reactions of guaiacol and alkyl guaiacol model compounds

Mannich reactions with guaiacols were first reported to occur at the para position relative to the phenolic hydroxyl group; they were later corrected to ortho regiochemistry based on melting point comparison between the dimethylamine Mannich base adduct and the diacetate of ortho-vanillin [95]. The utility of the reaction was extended to guaiacol derivatives [96], with reactions involving guaiacol and pyrocatechol showing varied yields with increasing chain length of the dialkylamine [97]. In this study, the condensation of a dialkylamine (either $NHMe_2$ or $NHEt_2$) with formaldehyde creates an electrophilic iminium species. The latter undergoes electrophilic aromatic substitution with the phenolate of guaiacol and alkyl guaiacols (Scheme 2). Compared to the synthesis of benzylamine from lignin-derived benzaldehydes [37], the Mannich reaction uses lower-cost reagents, has no side products, and requires less workup; solvent, residual formaldehyde and dialkylamine reagents, and one molar equivalent of water can be removed and recycled by simple distillation.

Though guaiacols contain adjacent electron-donating substituents, the phenol group is a stronger activator compared to the methoxy group. Mannich reactions with guaiacol yielded *ortho*- and *para*-substituted products (Scheme 2). Upon workup, the reaction of guaiacol and dimethylamine showed ^{13}C Nuclear Magnetic Resonance (NMR) signals for the NCH_2 group at δ = 62.2 and 64.1 ppm in approximately 2:1 area ratio (Fig. S6), corresponding to *ortho* (**1a**) and *para* (**1b**) addition to the phenol group. This 2:1 product ratio agreed well with the relative peak area ratios of the NCH_3 chemical shifts of **1a** (δ = 44.2) and **1b** (δ = 45.0). When guaiacol was reacted with diethylamine, approximately 1:1 of the *ortho* (**2a**): *para* (**2b**) substitution products were observed at δ = 56.7 and 57.6 ppm, respectively. These data suggest that additional steric bulk imparted by diethylamine favors substitution at the less hindered *para* position.

Mannich reactions with alkyl guaiacols yielded only *ortho*-substituted products with excellent yields (90–95%). For example, a reaction of methyl guaiacol, formaldehyde, and dimethylamine gave 2-((dimethylamino)methyl)-6-methoxy-4-methylphenol (**3**). A mass-to-charge ratio (*m/z*) of 195.14 [M^+] was observed by GC–MS, consistent with the molecular formula of $C_{11}H_{17}NO_2$. The ^{1}H NMR spectrum of **3** showed a singlet (δ = 3.48 ppm, 2H), characteristic of a methylene group of the newly added amine. This result was further confirmed by the corresponding ^{13}C resonance at 62.6 ppm. The NCH_3 protons of **3** appeared as a singlet (δ = 2.22 ppm, 6H) with the corresponding ^{13}C resonance observed at 44.2 ppm. An exact structure search found that compounds **1–5** have been previously reported [37,39,98–101]. The NMR data for previously unreported compounds **6–8** are summarized in Fig. S6.

To study the amination of lignin-derived guaiacols, silica gel chromatography was employed to isolate a 1:4:10 mixture of methyl guaiacol, ethyl guaiacol, and propyl guaiacol. Upon reacting with the Mannich conditions described for model compounds, desired phenolic amine products were observed from lignin-derived guaiacols by matching GC–MS retention times (RT) with authentic standards (Figs. S7–S8). Major products observed for reactions of lignin-derived guaiacols with dimethylamine included **3** (RT = 5.66 min, *m/z* obsd. = 194.13), **4** (RT = 6.03 min, *m/z* obsd. = 210.06), and **5** (RT = 6.39 min, *m/z* obsd. = 224.04). Major products observed for reactions of lignin-derived guaiacols with diethylamine included **6** (RT = 6.16 min, *m/z* obsd. = 224.16), **7** (RT = 6.34 min, *m/z* obsd. = 221.15), **8** (RT = 6.68 min, *m/z* obsd. = 235.14). Several of the *m/z* ratios observed in the lignin Mannich reactions represent ion fragments, such as loss of OH or OCH_3. It is noteworthy that reaction monitoring by GC–MS showed two major high molecular weight products (RT = 10.12 min, *m/z* = 330.24; RT = 10.97 min, *m/z* = 358.19) that may result from stable ions formed from lignin fragments. Since aldehyde resonances from phenolic formylation were not observed by IR or NMR of model compounds, 4-O-5′ radical coupling of alkyl guaiacols is unlikely [102]. Overall, the Mannich reaction used two molar equivalents each of amine and formaldehyde yielded near quantitative amounts of all lignin model compounds. However, when applied to purified lignin, 6 equivalents of amine and

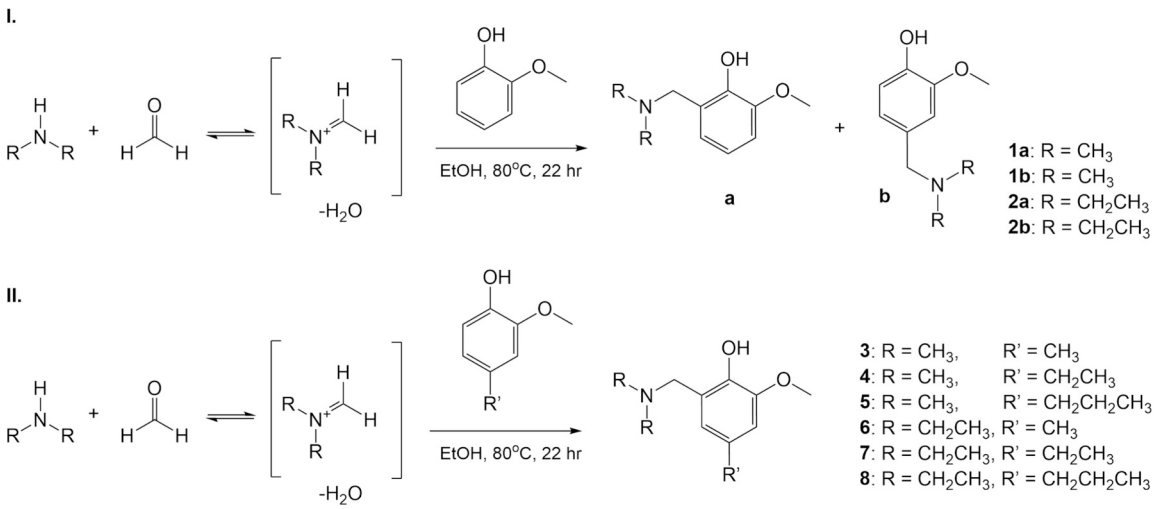

Scheme 2. Mechanism of Mannich reaction of formaldehyde, dialkylamines and guaiacols examined in this study. Iminium formation is followed by electrophilic aromatic substitution. I. Guaiacol reacts to form mixtures of *ortho* (**1a**, **2a**) and *para* (**1b**, **2b**) substituted products. II. 4-alkyl guaiacols react to exclusively form *ortho* products (**3–8**).

formaldehyde were required for complete amination, likely due to the presence of phenolic oligomers.

Additionally, ^{1}H and Distortionless Enhancement by Polarization Transfer (DEPT) NMR were performed on the depolymerized lignin product mixtures before and after the Mannich reaction with dimethylamine. The results show propyl guaiacol as the major depolymerization product, and compound **5** as the major Mannich product. Specifically, the newly installed methylene protons (Fig. S9) can be seen as 6H and 2H singlets at 2.3 and 3.6 ppm, respectively, consistent with the model compound. DEPT 45 and 135 spectra (Fig. S10) further confirmed the presence of the methylene group as respective positive and negative resonances at 62.6 ppm, also consistent with the model ^{13}C spectra for **5**.

3.4. Process economics and carbon footprint

Techno-economic analysis (TEA) and life-cycle assessment (LCA) were conducted based on experimental results to quantify production cost and carbon footprint of two different hypothetical lignin-based benzylamine facilities. The process models were developed for two production scales: 1) a state-of-the-art facility processing 75 t of kraft lignin per day, based on the scale of Domtar's LignoBoost plant in Fort Mill, SC, USA [103], and 2) a larger-scale facility processing 750 t per day, assuming lignin is sourced from multiple kraft pulping plants. At the state-of-art facility scale, benzylamines produced using MeOH exhibit lower costs ($132/kg - $254/kg) compared to those made with EtOH ($210/kg - $373/kg) and iPrOH ($300/kg - $535/kg) since MeOH is considerably cheaper than the other two alcohols [57] (Fig. 6). The lowest minimum selling price (MSP) for benzylamine among all cases ($132/kg, based on demonstrated performance in this study) is found when using MeOH alone.

Further coupling FA or Ru/C catalyst could improve lignin-to-monophenol yields but also increase final product cost, mainly depending on the yield achieved under different solvents. In MeOH solvent, the catalyst cost contribution exceeds that of FA addition, while in iPrOH solvent, the catalyst and FA costs are comparable. However, in

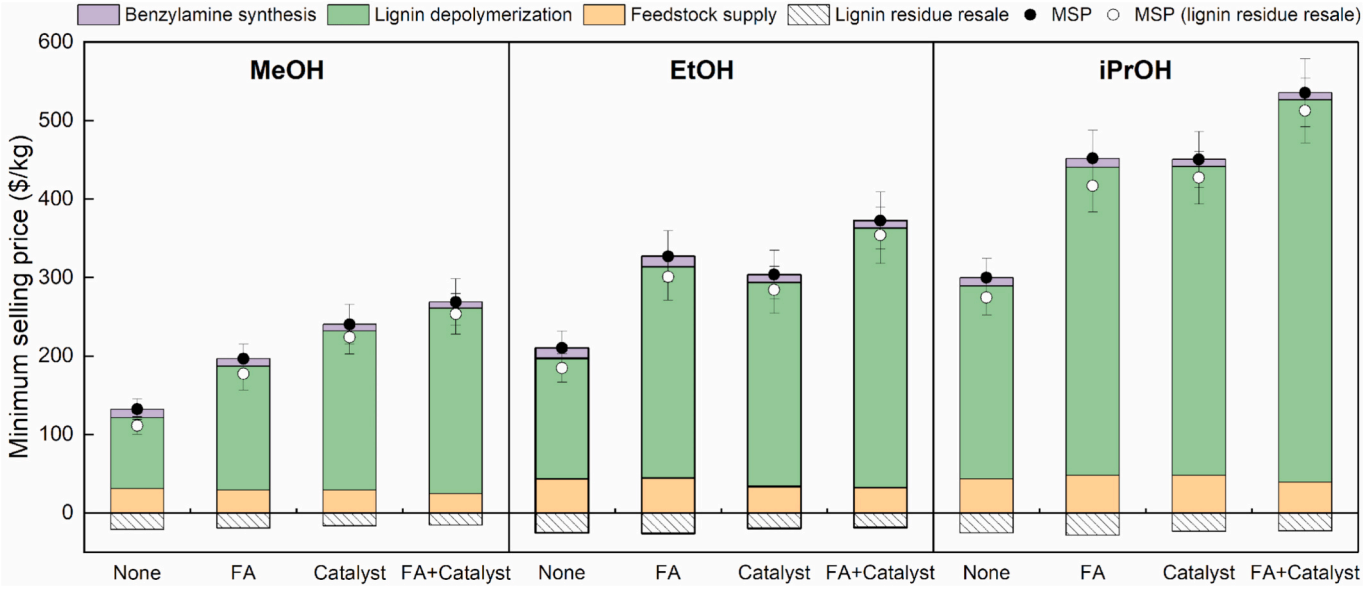

Fig. 6. Technoeconomic analysis results of a state-of-art benzylamine facility scale (75 t lignin/day) using three different solvents with and without FA and/or Ru/C (labeled as Catalyst).

the case of EtOH, adding FA contributes more to the overall cost than using Ru/C. Although the highest lignin-to-monophenol yield (6.5 wt%) is achieved using MeOH with FA and Ru/C, the overall economics of the MeOH-only case (with a yield of 4.9 wt%) outperform the highest-yield case. This is mainly due to the relatively high costs of FA and short lifetime associated with Ru/C. Notably, the cost can be further reduced if the solid residue after lignin depolymerization is collected resale as by-product. As illustrated in Fig. 6, we added a scenario assuming that these residues were sold into the bulk lignin market for applications such as soil amendment and energy generation. Hence, the MSPs of benzylamine could be reduced by \$16/kg - \$28/kg depending on the amount of remaining lignin, and the lowest MSP of benzylamine in the MeOH-only case could be further reduced to \$111/kg (Fig. 6).

Considering the MeOH's cost advantage, we further investigated opportunities for cost reduction at large-scale facilities using MeOH as the solvent. At a processing capacity of 750 t lignin per day, the lowest benzylamine MSP (\$105/kg) is still obtained in the case when MeOH is used without Ru/C or FA (Fig. 7A). Consistent with the state-of-art facility results, while incorporating FA increases monophenol yield by 14% (Fig. 3), it raises the benzylamine MSP by \$58/kg; alternatively, coupling Ru/C in the lignin depolymerization process nearly doubles the total benzylamine production cost compared to the MeOH-only scenario. Sensitivity analysis of the large-scale facility reveals that lignin depolymerization yield is the most influential cost driver across all scenarios (Fig. 7C–D). If the monophenol yield reaches its highest literature value [104], the benzylamine MSP could be reduced to approximately \$22/kg (Fig. 7C). Other inputs, such as kraft lignin prices, MeOH recycling rates, and Mannich reaction yields will greatly impact the economic feasibility of the facility.

The carbon footprint of the lignin-based benzylamine production at a large-scale facility was assessed to quantify the greenhouse gas (GHG) emissions associated with the process. To produce 1 kg of benzylamines, GHG results range from 26 kg CO_{2e} to 228 kg CO_{2e}. Similar to the cost results, adding FA and/or Ru/C catalyst enhances the lignin-to-monophenol yields, due to the high carbon footprint of FA production (~2 $kgCO_{2e}$/kg) and Ru/C (13.7 $kgCO_{2e}$/kg) [105], scenarios involving FA and/or Ru/C result in significantly higher GHG emissions compared to MeOH-only cases (Fig. 7B). Although utilizing catalysts or FA to increase lignin depolymerization yields is appealing from an experimental perspective, the associated costs and environmental burdens should be carefully considered as they can be substantially higher than those of solvent-only cases. If the depolymerized lignin residue is sold as a by-product, the net GHG emissions can be further reduced, as illustrated in Fig. 7B.

It is important to note that, due to the characteristic structural recalcitrance of kraft lignin, the product yields in this study were

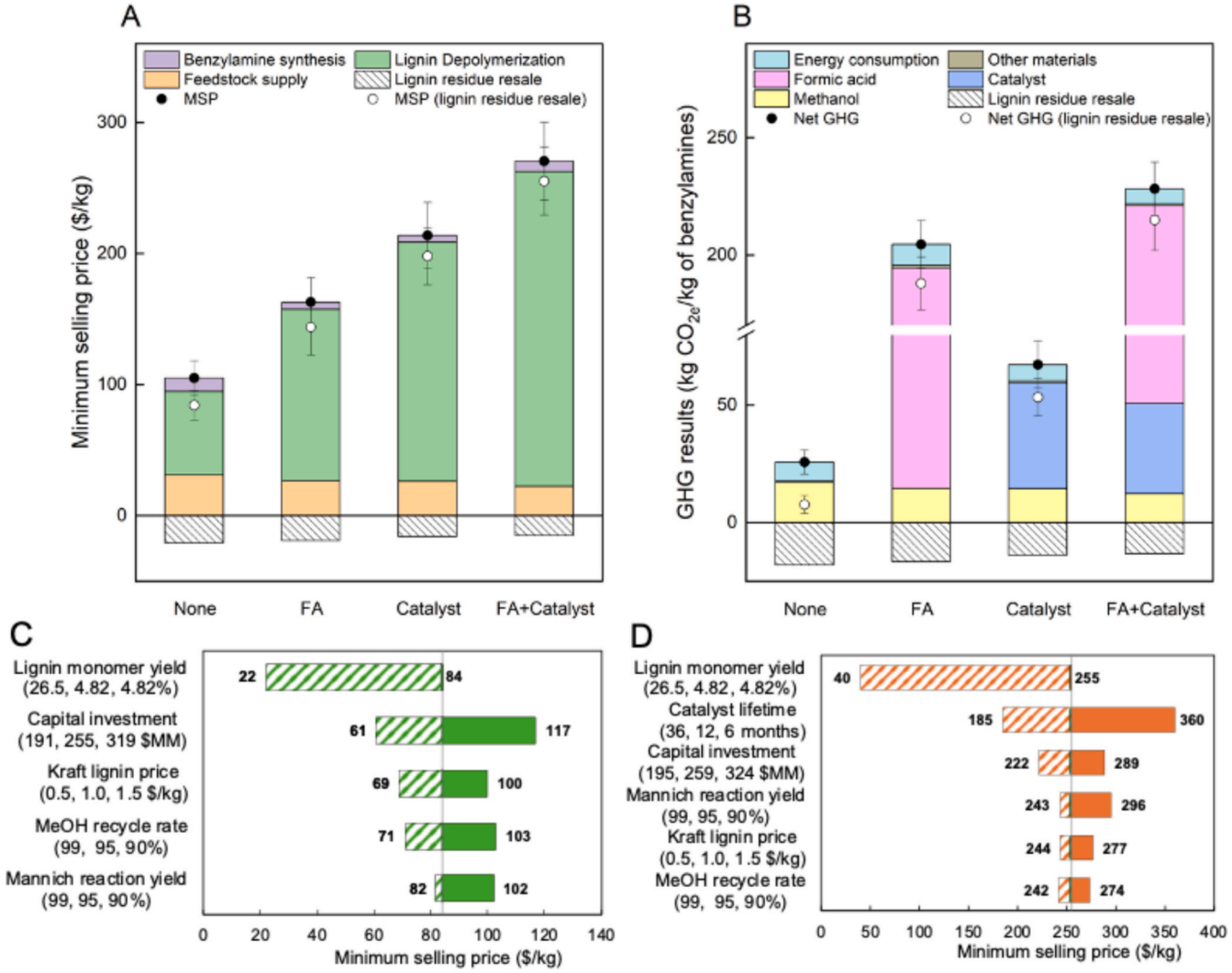

Fig. 7. A) TEA results and B) carbon footprint results of a large-scale benzylamine facility (750 t lignin processed per day) using MeOH with and without FA and/or Ru/C (labeled as Catalyst); C) sensitivity analysis results for a large-scale benzylamine facility using MeOH and D) sensitivity analysis results for a large-scale benzylamine facility using MeOH with FA and Ru/C.

relatively modest. For comparison, monomeric yields from lignin using Ru/C catalysts have been reported to reach 21% for organosolv lignin [87] and up to 51% for birch-derived lignin [23]. Nonetheless, our underlying chemistry is potentially transferable to other lignin sources (including other technical lignins, biofuel-process derived lignin, and natural lignin), to enable higher yields and enhance economic and emission performance.

4. Conclusions

We demonstrated the synthesis of functionalized benzylamines using monophenols derived from reductive lignin depolymerization. The selection of alcohol solvent was found to affect the monophenol product yield, but did not significantly impact the product distribution. Instead, incorporating FA and Ru/C in the reaction effectively shifted the product profile towards guaiacols with longer alkyl chains (e.g., propylguaiacol). Up to 6.5% of monophenols were obtained from commercial kraft softwood lignin using FA and Ru/C in methanol at 300 °C, 20 bar N_2 for 2 h. Thermodynamic modeling of activity coefficients, Gibbs solvation energy, and σ- potential revealed critical factors governing lignin dissolution and influencing its subsequent conversion. The observed product yields are hypothesized to result from superior solvency, acidity, and nucleophilicity of MeOH followed by EtOH and iPrOH. Amino alkylation of lignin-derived guaiacols to benzylamines was accomplished using the Mannich reaction with up to 95% yield. A technoeconomic analysis revealed that while lignin-to-monophenol yield is a key factor, other input parameters, such as Ru/C catalyst and reagent costs, also have substantial impacts in the economic viability of benzylamine production. Among the four lignin depolymerization systems investigated, the alcohol-only scenarios resulted in the lowest final product cost. The scenario with solely MeOH as the solvent was identified to be the most cost-effective, although this could shift if benzylamines with longer alkyl chains become more economically desirable. Note that lignin-derived benzylamines will require safety, toxicity, and application-specific assessments at later stages of product development to meet regulatory standards for final products. Functionalized benzylamines, with tunable alkyl chain lengths and oxygen functionalities inherited from different lignin-derived guaiacols, could unlock new properties and commercial applications. As an exploratory study, this work offers a unique perspective on transforming low-value lignin into high-value functionalized benzylamines, presenting a sustainable production pathway while addressing key economic and environmental challenges in biorefinery development.

CRediT authorship contribution statement

Chang Dou: Writing – review & editing, Writing – original draft, Visualization, Validation, Supervision, Project administration, Methodology, Investigation, Formal analysis, Data curation, Conceptualization. **Minliang Yang:** Writing – original draft, Visualization, Methodology, Investigation, Formal analysis, Data curation. **Nikhil Kumar:** Writing – original draft, Visualization, Methodology, Investigation, Formal analysis, Data curation. **Rolin A. Aguilar:** Investigation, Formal analysis, Data curation. **Addison J. Hitt:** Investigation, Formal analysis, Data curation. **Griffen Gonzalez:** Investigation, Formal analysis, Data curation. **Corinne D. Scown:** Writing – review & editing, Investigation. **Kenneth L. Sale:** Writing – review & editing, Methodology, Investigation. **Hemant Choudhary:** Writing – review & editing, Investigation. **Aaron M. Socha:** Writing – review & editing, Writing – original draft, Visualization, Methodology, Investigation, Funding acquisition, Formal analysis, Data curation, Conceptualization. **Ning Sun:** Writing – review & editing, Supervision, Resources, Project administration, Funding acquisition, Conceptualization.

Declaration of competing interest

The authors declare that they have no known competing financial interests or personal relationships that could have appeared to influence the work reported in this paper.

Acknowledgments

This research was funded through a Technology Commercialization Fund Award by the Bioenergy Technologies Office (BETO) within the US Department of Energy's (DOE) Office of Critical Minerals and Energy Innovation (CMEI). The technoeconomic analysis (TEA) and life-cycle assessment (LCA) work were partially funded by the USDA NIFA HATCH NC 02948. The authors would also like to thank Domtar Paper Co, LLC for providing the BioChoice® lignin and Dr. Elena Kreimer in College of Chemistry at the University of California, Berkeley for CHNS analysis. UC Berkeley D-Lab for advice in data analysis. We would also like to thank Bianca Susara, who helped to prepare the graphical abstract. The authors from the ABPDU acknowledge support from BETO and funding from the American Recovery and Reinvestment Act. This work was also supported by the Joint BioEnergy Institute, U.S. Department of Energy, Office of Science, Biological and Environmental Research Program under Award Number DE-AC02-05CH11231 with Lawrence Berkeley National Laboratory. Sandia National Laboratories is a multi-mission laboratory managed and operated by National Technology and Engineering Solutions of Sandia, LLC, a wholly-owned subsidiary of Honeywell International, Inc., for the U.S. Department of Energy's National Nuclear Security Administration under contract DE-NA0003525. This paper describes objective technical results and analysis. Any subjective views or opinions that might be expressed in the paper do not necessarily represent the views of the U.S. Department of Energy or the United States Government.

Appendix A. Supplementary data

Supplementary data to this article can be found online at https://doi.org/10.1016/j.cej.2026.174287.

Data availability

Data will be made available on request.

References

[1] V. Froidevaux, C. Negrell, S. Caillol, J.-P. Pascault, B. Boutevin, Biobased amines: from synthesis to polymers; present and future, Chem. Rev. 116 (2016) 14181–14224, https://doi.org/10.1021/acs.chemrev.6b00486.
[2] E. Blondiaux, J. Bomon, M. Smoleń, N. Kaval, F. Lemière, S. Sergeyev, L. Diels, B. Sels, B.U.W. Maes, Bio-based aromatic amines from lignin-derived monomers, ACS Sustain. Chem. Eng. 7 (2019) 6906–6916, https://doi.org/10.1021/acssuschemeng.8b06467.
[3] K. Natte, A. Narani, V. Goyal, N. Sarki, R.V. Jagadeesh, Synthesis of functional chemicals from lignin-derived monomers by selective organic transformations, Adv. Synth. Catal. 362 (2020) 5143–5169, https://doi.org/10.1002/adsc.202000634.
[4] S. Luan, W. Wu, B. Zheng, Y. Wu, M. Dong, X. Shen, T. Wang, Z. Deng, B. Zhang, B. Chen, X. Xing, H. Wu, H. Liu, B. Han, Atomically dispersed cobalt catalysts for tandem synthesis of primary benzylamines from oxidized β-O-4 segments, Chem. Sci. 15 (2024) 10954–10962, https://doi.org/10.1039/d4sc01813c.
[5] P.F. Vogt, J.J. Gerulis, Amines, Aromatic, in: Wiley-VCH (Ed.), Ullmann's Encyclopedia of Industrial Chemistry, Wiley, 2003, https://doi.org/10.1002/14356007.a02_037.
[6] Benzene, (chloromethyl)- - Substance Details - SRS | US EPA. https://cdxapps.epa.gov/oms-substance-registry-services/substance-details/19430. (Accessed 24 April 2025).
[7] M. Pelckmans, T. Renders, S. Van de Vyver, B.F. Sels, Bio-based amines through sustainable heterogeneous catalysis, Green Chem. 19 (2017) 5303–5331, https://doi.org/10.1039/C7GC02299A.
[8] D. Ruijten, T. Narmon, H. De Weer, R. van der Zweep, C. Poleunis, D.P. Debecker, B.U.W. Maes, B.F. Sels, Hydrogen borrowing: towards aliphatic tertiary amines from lignin model compounds using a supported copper catalyst, ChemSusChem 15 (2022) e202200868, https://doi.org/10.1002/cssc.202200868.

[9] B. Zhang, T. Guo, Y. Liu, F.E. Kühn, C. Wang, Z.K. Zhao, J. Xiao, C. Li, T. Zhang, Sustainable production of benzylamines from lignin, Angew. Chem. Int. Ed. 60 (2021) 20666–20671, https://doi.org/10.1002/anie.202105973.

[10] X. Dou, W. Li, C. Zhu, X. Jiang, Catalytic waste Kraft lignin hydrodeoxygenation to liquid fuels over a hollow Ni-Fe catalyst, Appl. Catal. B 287 (2021) 119975, https://doi.org/10.1016/j.apcatb.2021.119975.

[11] A.J. Ragauskas, G.T. Beckham, M.J. Biddy, R. Chandra, F. Chen, M.F. Davis, B. H. Davison, R.A. Dixon, P. Gilna, M. Keller, P. Langan, A.K. Naskar, J.N. Saddler, T.J. Tschaplinski, G.A. Tuskan, C.E. Wyman, Lignin valorization: improving lignin processing in the biorefinery, Science 344 (2014) 1246843, https://doi.org/10.1126/science.1246843.

[12] D.S. Bajwa, G. Pourhashem, A.H. Ullah, S.G. Bajwa, A concise review of current lignin production, applications, products and their environmental impact, Ind. Crop. Prod. 139 (2019) 111526, https://doi.org/10.1016/j.indcrop.2019.111526.

[13] V. Jassal, C. Dou, N. Sun, S. Singh, B.A. Simmons, H. Choudhary, Finding values in lignin: a promising yet under-utilized component of the lignocellulosic biomass, Front. Chem. Eng. 4 (2022), https://doi.org/10.3389/fceng.2022.1059305.

[14] D.D.S. Argyropoulos, C. Crestini, C. Dahlstrand, E. Furusjö, C. Gioia, K. Jedvert, G. Henriksson, C. Hulteberg, M. Lawoko, C. Pierrou, J.S.M. Samec, E. Subbotina, H. Wallmo, M. Wimby, Kraft lignin: a valuable, sustainable resource, opportunities and challenges, ChemSusChem 16 (2023) e202300492, https://doi.org/10.1002/cssc.202300492.

[15] E. Sjostrom, Wood Chemistry: Fundamentals and Applications, 2nd ed., Academic Press, 2013.

[16] L. Dessbesell, Z. Yuan, S. Hamilton, M. Leitch, R. Pulkki, C.C. Xu, Bio-based polymers production in a kraft lignin biorefinery: techno-economic assessment, Biofuels Bioprod. Biorefin. 12 (2018) 239–250, https://doi.org/10.1002/bbb.1834.

[17] Z. Sun, B. Fridrich, A. de Santi, S. Elangovan, K. Barta, Bright side of lignin depolymerization: toward new platform chemicals, Chem. Rev. 118 (2018) 614–678, https://doi.org/10.1021/acs.chemrev.7b00588.

[18] X. Liu, F.P. Bouxin, J. Fan, V.L. Budarin, C. Hu, J.H. Clark, Recent advances in the catalytic depolymerization of lignin towards phenolic chemicals: a review, ChemSusChem 13 (2020) 4296–4317, https://doi.org/10.1002/cssc.202001213.

[19] Y. Sang, H. Chen, M. Khalifeh, Y. Li, Catalysis and chemistry of lignin depolymerization in alcohol solvents - a review, Catal. Today 408 (2023) 168–181, https://doi.org/10.1016/j.cattod.2022.06.005.

[20] Q. Song, F. Wang, J. Cai, Y. Wang, J. Zhang, W. Yu, J. Xu, Lignin depolymerization (LDP) in alcohol over nickel-based catalysts via a fragmentation–hydrogenolysis process, Energ. Environ. Sci. 6 (2013) 994, https://doi.org/10.1039/c2ee23741e.

[21] D.S. Zijlstra, C.W. Lahive, C.A. Analbers, M.B. Figueirêdo, Z. Wang, C. S. Lancefield, P.J. Deuss, Mild organosolv lignin extraction with alcohols: the importance of benzylic alkoxylation, ACS Sustain. Chem. Eng. 8 (2020) 5119–5131, https://doi.org/10.1021/acssuschemeng.9b07222.

[22] C.S. Lancefield, I. Panovic, P.J. Deuss, K. Barta, N.J. Westwood, Pre-treatment of lignocellulosic feedstocks using biorenewable alcohols: towards complete biomass valorisation, Green Chem. 19 (2017) 202–214, https://doi.org/10.1039/C6GC02739C.

[23] S. Van den Bosch, W. Schutyser, R. Vanholme, T. Driessen, S.F. Koelewijn, T. Renders, B. De Meester, W.J.J. Huijgen, W. Dehaen, C.M. Courtin, B. Lagrain, W. Boerjan, B.F. Sels, Reductive lignocellulose fractionation into soluble lignin-derived phenolic monomers and dimers and processable carbohydrate pulps, Energ. Environ. Sci. 8 (2015) 1748–1763, https://doi.org/10.1039/C5EE00204D.

[24] R. Rinken, D. Posthuma, R. Rinaldi, Lignin stabilization and carbohydrate nature in H-transfer reductive catalytic fractionation: the role of solvent fractionation of lignin oil in structural profiling, ChemSusChem 16 (2023) e202201875, https://doi.org/10.1002/cssc.202201875.

[25] J. Zakzeski, P.C.A. Bruijnincx, A.L. Jongerius, B.M. Weckhuysen, The catalytic valorization of lignin for the production of renewable chemicals, Chem. Rev. 110 (2010) 3552–3599, https://doi.org/10.1021/cr900354u.

[26] J.K. Kenny, D.G. Brandner, S.R. Neefe, W.E. Michener, Y. Román-Leshkov, G. T. Beckham, J.W. Medlin, Catalyst choice impacts aromatic monomer yields and selectivity in hydrogen-free reductive catalytic fractionation, React, Chem. Eng. 7 (2022) 2527–2533, https://doi.org/10.1039/D2RE00275B.

[27] G.G. Facas, D.G. Brandner, J.R. Bussard, Y. Román-Leshkov, G.T. Beckham, Interdependence of solvent and catalyst selection on low pressure hydrogen-free reductive catalytic fractionation, ACS Sustain. Chem. Eng. 11 (2023) 4517–4522, https://doi.org/10.1021/acssuschemeng.2c07394.

[28] S. Inaba, Theoretical study of water cluster catalyzed decomposition of formic acid, J. Phys. Chem. A 118 (2014) 3026–3038, https://doi.org/10.1021/jp5021406.

[29] Y. Li, J. Li, B. Ren, H. Cheng, Conversion of lignin to nitrogenous chemicals and functional materials, Materials 17 (2024), https://doi.org/10.3390/ma17205110.

[30] B.G. Reed-Berendt, D.E. Latham, M.B. Dambatta, L.C. Morrill, Borrowing hydrogen for organic synthesis, ACS Cent. Sci. 7 (2021) 570–585, https://doi.org/10.1021/acscentsci.1c00125.

[31] A.M. Afanasenko, X. Wu, A. De Santi, W.A.M. Elgaher, A.M. Kany, R. Shafiei, M.-S. Schulze, T.F. Schulz, J. Haupenthal, A.K.H. Hirsch, K. Barta, Clean synthetic strategies to biologically active molecules from lignin: a green path to drug discovery, Angew. Chem. Int. Ed. 63 (2024) e202308131, https://doi.org/10.1002/anie.202308131.

[32] T. Yan, B.L. Feringa, K. Barta, Benzylamines via iron-catalyzed direct amination of benzyl alcohols, ACS Catal. 6 (2016) 381–388, https://doi.org/10.1021/acscatal.5b02160.

[33] X. Du, J. Li, M.E. Lindström, Modification of industrial softwood kraft lignin using Mannich reaction with and without phenolation pretreatment, Ind. Crop. Prod. 52 (2014) 729–735, https://doi.org/10.1016/j.indcrop.2013.11.035.

[34] T. Jayaramudu, K. Varaprasad, G. Adamus, J. Amber Jennings, J.D. Bumgardner, Mannich reaction: review of amine-functionalized lignin derivatives and their applications, Chem. Select 8 (2023), https://doi.org/10.1002/slct.202204451.

[35] C. Mannich, W. Krösche, Ueber ein kondensationsprodukt aus formaldehyd, ammoniak und antipyrin, Arch. Pharm. 250 (1912) 647–667, https://doi.org/10.1002/ardp.19122500151.

[36] M. Kollman, X. Jiang, S.J. Thompson, O. Mante, D.C. Dayton, H. Chang, H. Jameel, Improved understanding of technical lignin functionalization through comprehensive structural characterization of fractionated pine kraft lignins modified by the Mannich reaction, Green Chem. 23 (2021) 7122–7136, https://doi.org/10.1039/D1GC01842F.

[37] A.M. Socha, R. Parthasarathi, J. Shi, S. Pattathil, D. Whyte, M. Bergeron, A. George, K. Tran, V. Stavila, S. Venkatachalam, M.G. Hahn, B.A. Simmons, S. Singh, Efficient biomass pretreatment using ionic liquids derived from lignin and hemicellulose, Proc. Natl. Acad. Sci. U. S. A. 111 (2014) E3587–E3595, https://doi.org/10.1073/pnas.1405685111.

[38] B. Wang, T.-Y. Chen, H.-M. Wang, H.-Y. Li, C.-F. Liu, J.-L. Wen, Amination of biorefinery technical lignins using Mannich reaction synergy with subcritical ethanol depolymerization, Int. J. Biol. Macromol. 107 (2018) 426–435, https://doi.org/10.1016/j.ijbiomac.2017.09.012.

[39] A.B. McKague, Flocculating agnets derived from kraft lignin, J. Appl. Chem. 24 (2007) 607–615, https://doi.org/10.1002/jctb.2720241007.

[40] Y. Matsushita, S. Yasuda, Reactivity of a condensed–type lignin model compound in the Mannich reaction and preparation of cationic surfactant from sulfuric acid lignin, J. Wood Sci. 49 (2003) 166–171, https://doi.org/10.1007/s100860300026.

[41] V. Diez, A. DeWeese, R.S. Kalb, D.N. Blauch, A.M. Socha, Cellulose dissolution and biomass pretreatment using quaternary ammonium ionic liquids prepared from H-, G-, and S-type lignin-derived benzaldehydes and dimethyl carbonate, Ind. Eng. Chem. Res. (2019), https://doi.org/10.1021/acs.iecr.9b00640.

[42] S. Liu, L. Das, D.N. Blauch, C. Veronee, C. Dou, J. Gladden, N. Sun, A.M. Socha, Statistical design of experiments for production and purification of vanillin and aminophenols from commercial lignin, Green Chem. (2020), https://doi.org/10.1039/D0GC01234C.

[43] P. Tomani, The LignoBoost process, Cellul. Chem. Technol. 44 (2010) 53–58.

[44] O. Fearon, S. Kuitunen, K. Ruuttunen, V. Alopaeus, T. Vuorinen, Detailed modeling of kraft pulping chemistry. delignification, Ind. Eng. Chem. Res. 59 (2020) 12977–12985, https://doi.org/10.1021/acs.iecr.0c02110.

[45] T. Li, S. Takkellapati, The current and emerging sources of technical lignins and their applications, Biofuels Bioprod. Biorefin. 0 (2018) 1–32, https://doi.org/10.1002/bbb.1913.

[46] A. Riaz, D. Verma, H. Zeb, J.H. Lee, J.C. Kim, S.K. Kwak, J. Kim, Solvothermal liquefaction of alkali lignin to obtain a high yield of aromatic monomers while suppressing solvent consumption, Green Chem. 20 (2018) 4957–4974, https://doi.org/10.1039/C8GC02460J.

[47] A. Sluiter, B. Hames, R. Ruiz, C. Scarlata, J. Sluiter, D. Templeton, D. Crocker, Determination of Structural Carbohydrates and Lignin in Biomass: Laboratory Analytical Procedure (LAP), National Renewable Energy Laboratory, Golden, CO, 2008.

[48] Z. Hu, X. Du, J. Liu, H. Chang, H. Jameel, Structural characterization of pine kraft lignin: biochoice lignin vs indulin AT, J. Wood Chem. Technol. 36 (2016) 432–446, https://doi.org/10.1080/02773813.2016.1214732.

[49] J.H. Jang, A.R.C. Morais, M. Browning, D.G. Brandner, J.K. Kenny, L.M. Stanley, R.M. Happs, A.S. Kovvali, J.I. Cutler, Y. Román-Leshkov, J.R. Bielenberg, G. T. Beckham, Feedstock-agnostic reductive catalytic fractionation in alcohol and alcohol–water mixtures, Green Chem. 25 (2023) 3660–3670, https://doi.org/10.1039/D2GC04464A.

[50] M. Oregui-Bengoechea, I. Gandarias, P.L. Arias, T. Barth, Unraveling the role of formic acid and the type of solvent in the catalytic conversion of lignin: a holistic approach, ChemSusChem 10 (2017) 754–766, https://doi.org/10.1002/cssc.201601410.

[51] A. Klamt, Conductor-like screening model for real solvents: a new approach to the quantitative calculation of solvation phenomena, J. Phys. Chem. 99 (1995) 2224–2235, https://doi.org/10.1021/j100007a062.

[52] J.P. Perdew, Density-functional approximation for the correlation energy of the inhomogeneous electron gas, Phys. Rev. B 33 (1986) 8822–8824, https://doi.org/10.1103/PhysRevB.33.8822.

[53] A.D. Becke, Density-functional exchange-energy approximation with correct asymptotic behavior, Phys. Rev. A 38 (1988) 3098–3100, https://doi.org/10.1103/physreva.38.3098.

[54] F. Eckert, A. Klamt, Fast solvent screening via quantum chemistry: COSMO-RS approach, AICHE J. 48 (2002) 369–385, https://doi.org/10.1002/aic.690480220.

[55] M. Gonzalez-Miquel, M. Massel, A. DeSilva, J. Palomar, F. Rodriguez, J. F. Brennecke, Excess enthalpy of monoethanolamine + ionic liquid mixtures: how good are COSMO-RS predictions? J. Phys. Chem. B 118 (2014) 11512–11522, https://doi.org/10.1021/jp507547q.

[56] J. Reinisch, A. Klamt, F. Eckert, M. Diedenhofen, Prediction of the temperature dependence of a polyether–water mixture using COSMOtherm, Fluid Phase Equilib. 310 (2011) 7–10, https://doi.org/10.1016/j.fluid.2011.05.015.

[57] C. Nait Saidi, D.C. Mielczarek, P. Paricaud, Predictions of solvation Gibbs free energies with COSMO-SAC approaches, Fluid Phase Equilib. 517 (2020) 112614, https://doi.org/10.1016/j.fluid.2020.112614.

[58] J.M. Prausnitz, R.N. Lichtenthaler, E.G. De Azevedo, Molecular thermodynamics of fluid-phase equilibria, Pearson Education, 1998.

[59] D. Humbird, R. Davis, L. Tao, C. Kinchin, D. Hsu, A. Aden, P. Schoen, J. Lukas, B. Olthof, M. Worley, D. Sexton, D. Dudgeon, Process Design and Economics for Biochemical Conversion of Lignocellulosic Biomass to Ethanol: Dilute-acid Pretreatment and Enzymatic Hydrolysis of Corn Stover, National Renewable Energy Laboratory (NREL), Golden, CO (United States), 2011, https://doi.org/10.2172/1013269.

[60] A. Kloekhorst, Y. Shen, Y. Yie, M. Fang, H.J. Heeres, Catalytic hydrodeoxygenation and hydrocracking of Alcell® lignin in alcohol/formic acid mixtures using a Ru/C catalyst, Biomass Bioenergy 80 (2015) 147–161, https://doi.org/10.1016/j.biombioe.2015.04.039.

[61] R.-C. Sun, Lignin source and structural characterization, ChemSusChem 13 (2020) 4385–4393, https://doi.org/10.1002/cssc.202001324.

[62] C. Chio, M. Sain, W. Qin, Lignin utilization: a review of lignin depolymerization from various aspects, Renew. Sustain. Energy Rev. 107 (2019) 232–249, https://doi.org/10.1016/j.rser.2019.03.008.

[63] A. Agarwal, M. Rana, J.-H. Park, Advancement in technologies for the depolymerization of lignin, Fuel Process. Technol. 181 (2018) 115–132, https://doi.org/10.1016/j.fuproc.2018.09.017.

[64] J. Cai, Md.M. Rahman, S. Zhang, M. Sarker, X. Zhang, Y. Zhang, X. Yu, E.H. Fini, Review on aging of bio-oil from biomass pyrolysis and strategy to slowing aging, Energy Fuel 35 (2021) 11665–11692, https://doi.org/10.1021/acs.energyfuels.1c01214.

[65] M.M. Abu-Omar, K. Barta, G.T. Beckham, J.S. Luterbacher, J. Ralph, R. Rinaldi, Y. Román-Leshkov, J.S.M. Samec, B.F. Sels, F. Wang, Guidelines for performing lignin-first biorefining, Energ. Environ. Sci. 14 (2021) 262–292, https://doi.org/10.1039/D0EE02870C.

[66] D. Bourbiaux, J. Pu, F. Rataboul, L. Djakovitch, C. Geantet, D. Laurenti, Reductive or oxidative catalytic lignin depolymerization: an overview of recent advances, Catal. Today 373 (2021) 24–37, https://doi.org/10.1016/j.cattod.2021.03.027.

[67] Z. Wu, Y. Jiang, X. Wang, J. Xu, L. Hu, A review on the separation of lignin depolymerized products, Biomass Convers. Biorefinery (2022), https://doi.org/10.1007/s13399-021-02266-3.

[68] W. Schutyser, S. Van den Bosch, T. Renders, T. De Boe, S.F. Koelewijn, A. Dewaele, T. Ennaert, O. Verkinderen, B. Goderis, C.M. Courtin, B.F. Sels, Influence of bio-based solvents on the catalytic reductive fractionation of birch wood, Green Chem. 17 (2015) 5035–5045, https://doi.org/10.1039/C5GC01442E.

[69] T. Renders, S. Van den Bosch, T. Vangeel, T. Ennaert, S.-F. Koelewijn, G. Van den Bossche, C.M. Courtin, W. Schutyser, B.F. Sels, Synergetic effects of alcohol/water mixing on the catalytic reductive fractionation of poplar wood, ACS Sustain. Chem. Eng. 4 (2016) 6894–6904, https://doi.org/10.1021/acssuschemeng.6b01844.

[70] H. Choudhary, L. Das, J.G. Pelton, L. Sheps, B.A. Simmons, J.M. Gladden, S. Singh, Funneled depolymerization of ionic liquid-based biorefinery "Heterogeneous" lignin into guaiacols over reusable palladium catalyst, Chem. A Eur. J. 29 (2023) e202300330, https://doi.org/10.1002/chem.202300330.

[71] D.H. Ripin, D.A. Evans, Evan's pKa Table, 2005 (n.d.).

[72] S. Huang, N. Mahmood, M. Tymchyshyn, Z. Yuan, C.C. Xu, Reductive depolymerization of kraft lignin for chemicals and fuels using formic acid as an in-situ hydrogen source, Bioresour. Technol. 171 (2014) 95–102, https://doi.org/10.1016/j.biortech.2014.08.045.

[73] Z. Wu, X. Zhao, J. Zhang, X. Li, Y. Zhang, F. Wang, Ethanol/1,4-dioxane/formic acid as synergistic solvents for the conversion of lignin into high-value added phenolic monomers, Bioresour. Technol. 278 (2019) 187–194, https://doi.org/10.1016/j.biortech.2019.01.082.

[74] L. Das, M. Li, J. Stevens, W. Li, Y. Pu, A.J. Ragauskas, J. Shi, Characterization and catalytic transfer hydrogenolysis of deep eutectic solvent extracted sorghum lignin to phenolic compounds, ACS Sustain. Chem. Eng. 6 (2018) 10408–10420, https://doi.org/10.1021/acssuschemeng.8b01763.

[75] W. Wang, Y. Fu, Y. Chen, H. Miao, H. Zheng, J. Pan, Z. Wang, Y. Liu, W. Jiang, Microwave depolymerization of lignin via dynamic vapor flow reaction system: HCOOH as pretreatment solvent or reforming solvent vapor, ChemSusChem 17 (2024) e202400151, https://doi.org/10.1002/cssc.202400151.

[76] W. Xie, B. Hu, Y. Xia, G. Song, J. Liu, Y. Liu, Q. Lu, A novel insight into the bimolecular concerted interaction in lignin pyrolysis: Tautomer-assisted hydrogen transfer mechanism, Chem. Eng. J. 463 (2023) 142513, https://doi.org/10.1016/j.cej.2023.142513.

[77] A. Toledano, L. Serrano, J. Labidi, A. Pineda, A.M. Balu, R. Luque, Heterogeneously catalysed mild hydrogenolytic depolymerisation of lignin under microwave irradiation with hydrogen-donating solvents, ChemCatChem 5 (2013) 977–985, https://doi.org/10.1002/cctc.201200616.

[78] A. Rahimi, A. Ulbrich, J.J. Coon, S.S. Stahl, Formic-acid-induced depolymerization of oxidized lignin to aromatics, Nature 515 (2014) 249–252, https://doi.org/10.1038/nature13867.

[79] S. Qu, Y. Dang, C. Song, J. Guo, Z.-X. Wang, Depolymerization of oxidized lignin catalyzed by formic acid exploits an unconventional elimination mechanism involving 3c–4e bonding: A DFT mechanistic study, ACS Catal. 5 (2015) 6386–6396, https://doi.org/10.1021/acscatal.5b01095.

[80] X. Dou, W. Li, C. Zhu, X. Jiang, H. Chang, H. Jameel, Cleavage of aryl–ether bonds in lignin model compounds using a Co–Zn-beta catalyst, RSC Adv. 10 (2020) 43599–43606, https://doi.org/10.1039/D0RA08121C.

[81] ÿzlem Z. firin, O. Demirkol, D. Akbaflar, E.S. Giray, Clean and efficient synthesis of flavanone in sub-critical water, J. Supercrit. Fluids 81 (2013) 217–220, https://doi.org/10.1016/j.supflu.2013.05.014.

[82] P.W. Atkins, J. De Paula, The response of equilibria to temperature, in: Physical Chemistry, 2006.

[83] I. Kristianto, S.O. Limarta, H. Lee, J.-M. Ha, D.J. Suh, J. Jae, Effective depolymerization of concentrated acid hydrolysis lignin using a carbon-supported ruthenium catalyst in ethanol/formic acid media, Bioresour. Technol. 234 (2017) 424–431, https://doi.org/10.1016/j.biortech.2017.03.070.

[84] S. Huang, N. Mahmood, Y. Zhang, M. Tymchyshyn, Z. Yuan, C. (Charles) Xu, Reductive de-polymerization of kraft lignin with formic acid at low temperatures using inexpensive supported Ni-based catalysts, Fuel 209 (2017) 579–586, https://doi.org/10.1016/j.fuel.2017.08.031.

[85] M. Kleinert, T. Barth, Phenols from lignin, Chem. Eng. Technol. 31 (2008) 736–745, https://doi.org/10.1002/ceat.200800073.

[86] X. Besse, Y. Schuurman, N. Guilhaume, Hydrothermal conversion of lignin model compound eugenol, Catal. Today 258 (2015) 270–275, https://doi.org/10.1016/j.cattod.2014.12.010.

[87] Z. Shen, C. Shi, F. Liu, W. Wang, M. Ai, Z. Huang, X. Zhang, L. Pan, J.-J. Zou, Advances in heterogeneous catalysts for lignin hydrogenolysis, Adv. Sci. 11 (2024) e2306693, https://doi.org/10.1002/advs.202306693.

[88] C. Zhang, X. Shen, Y. Jin, J. Cheng, C. Cai, F. Wang, Catalytic strategies and mechanism analysis orbiting the center of critical intermediates in lignin depolymerization, Chem. Rev. 123 (2023) 4510–4601, https://doi.org/10.1021/acs.chemrev.2c00664.

[89] R. Shu, Y. Xu, L. Ma, Q. Zhang, C. Wang, Y. Chen, Controllable production of guaiacols and phenols from lignin depolymerization using Pd/C catalyst cooperated with metal chloride, Chem. Eng. J. 338 (2018) 457–464, https://doi.org/10.1016/j.cej.2018.01.002.

[90] R. Ma, W. Hao, X. Ma, Y. Tian, Y. Li, Catalytic ethanolysis of Kraft lignin into high-value small-molecular chemicals over a nanostructured α-molybdenum carbide catalyst, Angew. Chem. Int. Ed. 53 (2014) 7310–7315, https://doi.org/10.1002/anie.201402752.

[91] I. Domínguez, B. Gonzalez, B. Orge, C. Held, M. Voges, E.A. Macedo, Activity coefficients at infinite dilution for different alcohols and ketones in [EMpy][ESO4]: experimental data and modeling with PC-SAFT, Fluid Phase Equilib. 424 (2016) 32–40, https://doi.org/10.1016/j.fluid.2015.09.003.

[92] K. Aidas, C. Angeli, K.L. Bak, V. Bakken, R. Bast, L. Boman, O. Christiansen, R. Cimiraglia, S. Coriani, P. Dahle, E.K. Dalskov, U. Ekström, T. Enevoldsen, J. J. Eriksen, P. Ettenhuber, B. Fernández, L. Ferrighi, H. Fliegl, L. Frediani, K. Hald, A. Halkier, C. Hättig, H. Heiberg, T. Helgaker, A.C. Hennum, H. Hettema, E. Hjertenæs, S. Høst, I.-M. Høyvik, M.F. Iozzi, B. Jansík, H.J.A. Jensen, D. Jonsson, P. Jørgensen, J. Kauczor, S. Kirpekar, T. Kjærgaard, W. Klopper, S. Knecht, R. Kobayashi, H. Koch, J. Kongsted, A. Krapp, K. Kristensen, A. Ligabue, O.B. Lutnæs, J.I. Melo, K.V. Mikkelsen, R.H. Myhre, C. Neiss, C. B. Nielsen, P. Norman, J. Olsen, J.M.H. Olsen, A. Osted, M.J. Packer, F. Pawlowski, T.B. Pedersen, P.F. Provasi, S. Reine, Z. Rinkevicius, T.A. Ruden, K. Ruud, V.V. Rybkin, P. Sałek, C.C.M. Samson, A.S. de Merás, T. Saue, S.P. A. Sauer, B. Schimmelpfennig, K. Sneskov, A.H. Steindal, K.O. Sylvester-Hvid, P. R. Taylor, A.M. Teale, E.I. Tellgren, D.P. Tew, A.J. Thorvaldsen, L. Thøgersen, O. Vahtras, M.A. Watson, D.J.D. Wilson, M. Ziolkowski, H. Agren, The Dalton quantum chemistry program system, Wiley Interdiscip. Rev. Comput. Mol. Sci. 4 (2014) 269–284, https://doi.org/10.1002/wcms.1172.

[93] Y. Su, C. Xu, J. Liu, Z. Liu, Electrooxidation of 2-propanol compared ethanol on Pd electrode in alkaline medium, J. Power Sources 194 (2009) 295–297, https://doi.org/10.1016/j.jpowsour.2009.04.076.

[94] H. Dai, Q. Cui, Z. Wang, C. Zhai, Sustainable hydrogen production through coupling isopropanol-butanol-ethanol with enhanced heat recirculation, Int. J. Hydrogen Energy 50 (2024) 547–560, https://doi.org/10.1016/j.ijhydene.2023.09.283.

[95] E.L. Eliel, The structure of the guaiacol "mannich bases,", J. Am. Chem. Soc. 73 (1951) 43–45, https://doi.org/10.1021/ja01145a017.

[96] H. Mikawa, K. Sato, C. Takasaki, K. Ebisawa, Studies on the cooking mechanism of wood. XV. mannich reaction on lignin model compounds and the estimation of the amount of the simple guaiacyl nucleus in thiolignin, Bull. Chem. Soc. Jpn. 29 (1956) 259–265, https://doi.org/10.1246/bcsj.29.259.

[97] M.J. Caulfield, T. Russo, D.H. Solomon, Controlled synthesis of novel dibenzene-1,2-diol Mannich bases, Aust. J. Chem. 53 (2000) 545–549.

[98] F.X. Perrin, J. Pagetti, Synthesis, characterization, and electropolymerization of Mannich bases: influence of substituents on protective ability of organic coatings, J. Appl. Polym. Sci. 75 (2000) 1054–1067.

[99] T. Dutta, J. Sun, B.A. Simmons, S. Singh, Conversion of lignin to ionic liquid, US11254637B2 / WO2017214334, 2017.

[100] A.P. Degnan, A.I. Meyers, Total syntheses of (−)-Herbertenediol, (−)-Mastigophorene A, and (−)-Mastigophorene B. Combined utility of chiral bicyclic lactams and chiral aryl oxazolines, J. Am. Chem. Soc. 121 (1999) 2762–2769, https://doi.org/10.1021/ja984182x.

[101] K.B. Weissert, M. Hochegger, F. Bálint, Novel amine-n-oxide compounds, WO2023046768, 2023.

[102] N. Giummarella, I.V. Pylypchuk, O. Sevastyanova, M. Lawoko, New structures in *Eucalyptus* kraft lignin with complex mechanistic implications, ACS Sustain. Chem. Eng. (2020), https://doi.org/10.1021/acssuschemeng.0c03776.

[103] Valmet, LignoBoost plant at Domtar's Plymouth mill in North Carolina. https://www.valmet.com/about-us/references/pulping-and-fiber/lignoboost-plant-at-domtars-plymouth-mill-in-north-carolina/, 2015. (Accessed 16 May 2025).
[104] M. Chen, Z. Tang, Y. Wang, J. Shi, C. Li, Z. Yang, J. Wang, Catalytic depolymerization of Kraft lignin to liquid fuels and guaiacol over phosphorus modified Mo/Sepiolite catalyst, Chem. Eng. J. 427 (2022) 131761, https://doi.org/10.1016/j.cej.2021.131761.
[105] L.J. Snowden-Swan, K.A. Spies, G.J. Lee, Y. Zhu, Life cycle greenhouse gas emissions analysis of catalysts for hydrotreating of fast pyrolysis bio-oil, Biomass Bioenergy 86 (2016) 136–145, https://doi.org/10.1016/j.biombioe.2016.01.019.